

Parallelism in Endocarp Form Sheds Light on Fruit Syndrome Evolution in *Viburnum*

Wendy L. Clement,^{1,3} Theodore J. Stammer,¹ Amanda Goble,¹ Patrick Gallagher,¹ and Michael J. Donoghue²

¹Department of Biology, The College of New Jersey, 2000 Pennington Road, Ewing, New Jersey, 08628 USA; clementw@tcnj.edu; tjstammer@gmail.com; goblea1@tcnj.edu; gallagp@tcnj.edu

²Department of Ecology and Evolutionary Biology, Yale University, PO Box 208106, New Haven, Connecticut 06520, USA; michael.donoghue@yale.edu

³Author for correspondence (clementw@tcnj.edu)

Communicating Editor: Annah Moteetee

Abstract—All *Viburnum* species produce drupes with a hardened endocarp surrounding a single seed. Endocarp form varies greatly within *Viburnum*, and differences in shape have long been used to distinguish major subclades. Here we trace the evolution of *Viburnum* endocarp shape using morphometric analyses and phylogenies for 115 *Viburnum* species. Endocarp measurements were obtained from fruits sampled from herbarium specimens and from field collections, and shapes were analyzed using elliptical Fourier analysis. We infer that the first *viburnums* had flattened and grooved endocarps. Subsequently, there were multiple losses of grooving in conjunction with shifts to both highly flattened and nearly round endocarps. In several clades the parallel evolution of a derived endocarp shape was accompanied by changes in a suite of other fruit traits, yielding distinctive fruit syndromes likely related to bird dispersal. However, in other clades endocarp shapes similar to the ancestral form have been retained while other fruit traits (color, amount of flesh, nutritional content) have diverged. We quantify cases of parallel evolution in endocarp shape that cut across recognized fruit syndromes such as red, carbohydrate-rich fruits with flattened endocarps or blue, lipid-rich fruits with round endocarps. Our analyses now invite studies of function and the selective factors that have yielded the distinctive suites of fruit and seed traits that distinguish the major *Viburnum* lineages.

Keywords—Elliptical Fourier analysis, morphometrics, phylogeny.

The enormous diversity of fruit types has long been tied to the evolution of seed dispersal strategies. Animal dispersal, involving frugivorous birds and mammals (endozoochory), is practically synonymous with the production of fleshy propagules (Van der Pijl 1969). Variation among fleshy fruits with respect to color, texture, nutrition, and shape is determined by differences in the pericarp layers surrounding the seed. One type of fleshy fruit is the drupe, which generally has a single seed surrounded by a hardened endocarp that is differentiated from the fleshy layers. For plants with endocarps, this forms an additional protective layer around the seed (Dardick and Callahan 2014). While the precise role of endocarp morphology in relation to seed protection, dispersal, and germination is largely unknown, various conditions of the endocarp, including overall size and thickness, have been shown to affect seed removal and dispersal (Zhang and Zhang 2008). Aside from their functional significance, endocarp shapes have been important in taxonomic studies and in delimiting species and clades (e.g. Plunkett et al. 1996; Sattarian and van der Maesen 2006; Depypere et al. 2007; Wefferling et al. 2013; Koubouris et al. 2019). Likewise, fossilized endocarps are of great interest to paleobotanists for identification purposes (e.g. Dilcher and McQuade 1967; Boon et al. 1989; Rozefelds and Christophel 1996; Gottschling et al. 2002; Li et al. 2011). Yet, despite this interest from various quarters, there have been few detailed quantitative and comparative studies of endocarps and associated fruit traits conducted in a phylogenetic context.

Viburnum L. is a clade of approximately 165 species characterized by drupes that range in mature color from yellow to red to blue to black (Fig. 1). In his worldwide treatment of *Viburnum* in 1861, Oersted highlighted the value of endocarp shape in distinguishing between major groups of species, some of which he recognized at the time as separate genera. These distinctions have been well appreciated in more recent treatments (Rehder 1940; Hara 1983; Donoghue 1983a, 1983b; Yang and Malécot 2011). Jacobs et al. (2008) provided the first evolutionary perspective on endocarp morphology in *Viburnum*,

identifying five broad categories of grooving. Using a phylogeny of the 17 species that were studied in detail, they inferred multiple transitions from an endocarp shape with grooving to a flattened or to a spherical endocarp with little or no grooving (Jacobs et al. 2008). Since then there have been significant improvements in our understanding of *Viburnum* phylogeny. A concerted effort to increase sampling and resolution, using a greatly expanded set of genetic markers, has resulted in a tree that includes one or more samples of nearly all ~165 species (Clement and Donoghue 2011; Clement et al. 2014; Spriggs et al. 2015; Landis et al. 2020). Additionally, an analysis of a suite of *Viburnum* fruit traits in a phylogenetic framework has documented the repeated evolution of two distinct ‘fruit syndromes’ (Sinnott-Armstrong et al. 2020). One syndrome includes species with blue fruit color, low moisture yet lipid-rich pulp, and rounded endocarps. The other major syndrome includes red-fruited species with high moisture yet carbohydrate-rich pulp, and flattened endocarps (Sinnott-Armstrong et al. 2020). This study documented correlations between basic endocarp shape (length and width measurements) and other fruit traits, but subtle differences in grooving patterns and overall endocarp form were not explored.

Here we further the study of endocarp evolution in *Viburnum* by incorporating 70% of extant species diversity. Treating endocarp shape as a continuous character and employing a tree-based analysis of convergence, we explore endocarp shape evolution in the context of a far more complete *Viburnum* phylogeny. We relate our findings to previous studies of endocarp morphology (Jacobs et al. 2008), revisit the fruit dispersal syndromes of Sinnott-Armstrong et al. (2020), and consider the significance of endocarp shape for *Viburnum* taxonomy.

MATERIALS AND METHODS

Sampling—To examine variation in endocarp shape, we sampled 122 of the ca. 165 species of *Viburnum*, covering all major subclades (Appendix 1). Endocarps were sampled from dried and pickled fruits from field collections (P.W. Sweeney, W.L. Clement, and M.J. Donoghue) as well as dried

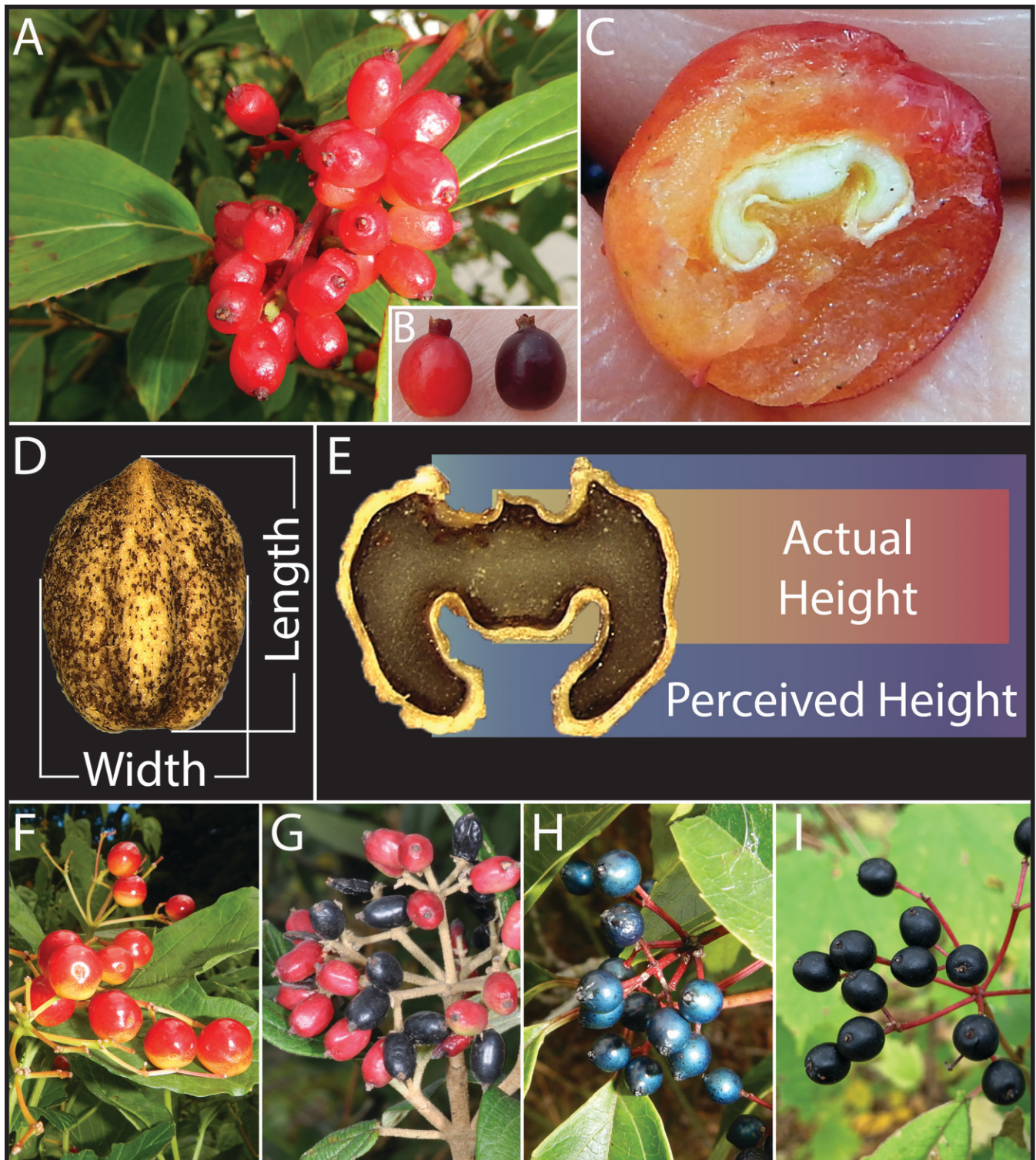


FIG. 1. Fruit and endocarp morphology in *Viburnum*. A. Infructescence of *V. erubescens* (Solenotinus). B. At maturity, the red fruits of *V. erubescens* turn black one at a time (sequential color development). C. Cross section of a *V. erubescens* fruit showing the endocarp and the white endosperm of the seed within. D. Width and length measurements made on whole endocarps. E. Two different height measurements taken from endocarps in cross-section: 'actual' height (red rectangle) and 'perceived' height (blue rectangle). F–I. Variation in *Viburnum* fruit color. F. Synchronous maturation of *V. opulus* fruits from yellow to red. G. Sequential maturation of the fruits of *V. chinshanense* from red to black. H. Metallic blue fruits of *V. propinquum*. I. Black fruits of *V. acerifolium*. Photo credits: M. J. Donoghue A–C, F, H, I; P. W. Sweeney G.

fruits from herbarium sheets at A, GH, and YU. Four species, from distantly related lineages within *Viburnum*, were chosen to explore intraspecific variation in endocarp shape: *V. dentatum* L. (Dentata), *V. prunifolium* L. (Lentago), *V. dilatatum* Thunb. (Succotinus), and *V. acerifolium* L. (Lobata). Approximately 10 fruits from each of five individuals were sampled for a

total of 50 fruits per focal species. Fruits were sampled from The College of New Jersey, Ewing, New Jersey; the main campus of Yale University, New Haven, Connecticut; the Marsh Botanical Garden of Yale University, New Haven, Connecticut; and the Nayfield Preserve, Hopewell Township, New Jersey.

Our phylogenetic analysis of *Viburnum* included 115 of the 122 species for which endocarp data were collected. The seven species for which shape data were collected but insufficient molecular data were available are *V. fordiae* Hance, *V. hondurense* Standl., *V. ovatifolium* Rehder, *V. tengyuehense* (W.W.Sm.) P.S.Hsu, *V. ternatum* Rehder, *V. tiliaefolium* (Oerst.) Hemsl., and *V. tsangii* Rehder. Here we highlight our most recent *Viburnum* phylogeny based on cpDNA and nrITS sequences (see Landis et al. 2020). We also carried out all relevant analyses using a tree based largely on RAD-seq data (Landis et al. 2020). Although the tree topologies obtained in these analyses are similar in most respects, there are some important differences listed below, including alternative placements of *V. clemensiae* J.Kern, which has often been placed as sister to all other viburnums based largely on cpDNA data (Clement et al. 2014; Spriggs et al. 2015; but see Lens et al. 2016). For comparability, we pruned the Landis et al. (2020) RADseq-based tree to include the same 115 taxa as the cpDNA + nrITS dataset. All morphological data matrices and trees are available in Dryad (Clement et al. 2021).

Sample Preparation and Imaging—As the endocarp is a hard, fibrous structure surrounding the seed, its form is well preserved on herbarium specimens from which the majority of our data were collected. Measurements of endocarps were made directly from digital images of herbarium and pickled collections using a Leica stereoscope outfitted with a 3.1 megapixel digital camera or from camera lucida drawings of dried endocarps. For pickled material, the exocarp and mesocarp were manually stripped from the fruit to expose the endocarp. For herbarium specimens, the fruit pulp generally dries to a relatively thin layer around the endocarp and is easily removed or distinguished by its color and texture from the endocarp. Endocarps were first photographed lying flat (i.e. with both the apex and base in view). The endocarps were then cut in cross section using a razor blade, positioned upright in clay and photographed in cross section with the dorsal side toward the top of the image. Camera lucida drawings representing the same set of photographs were drawn at a $9 \times$ scale (except *V. lentago* drawn at $6 \times$) and digitized to facilitate measuring. The dorsal and ventral sides of a *Viburnum* endocarp can readily be established in cross section by reference to a prominent vascular bundle (the “central bundle” of Wilkinson 1948) that runs from the bottom to the top of the ovary through the center of the mesocarp along the ventral side.

Measurements of Endocarp Shape—Measurements were taken from the digital images and camera lucida drawings using ImageJ (Abramoff et al. 2004) and Leica Application Suite X (LASX) software (Leica Microsystems, Buffalo Grove, Illinois). ‘Length’ was measured as the distance from the apex to the farthest point at the base of the endocarp (Fig. 1D). ‘Width’ was measured as the distance between the farthest points along the lateral axis of the endocarp (Fig. 1D). As many endocarp shapes have a prominent ventral groove in their cross section, which effectively creates lateral “arms” of the endocarp that appear to curve and create a horseshoe shape (e.g. *Solenotinus*, Fig. 1C), we collected two different ‘height’ measurements. The first, ‘perceived height,’ was measured as the distance between the farthest points from the dorsal to the ventral side of the endocarp, i.e. taking into account any curvature (Fig. 1E). Then, ‘actual height’ was measured as the distance in the center of the cross section of the endocarp from the dorsal to the ventral side, i.e. ignoring any lateral curvature (Fig. 1E). In an endocarp that is flattened and not curved around a central groove, the perceived and the actual heights could be the same. The distribution of endocarp shape was examined using a scatterplot generated using R statistical software (R Core Team 2019), comparing the width/perceived height ratio against the length of the endocarp.

To calculate an approximate volume of an endocarp, we considered the shape to be best represented by an ellipsoid. We then applied the formula to calculate the volume of an ellipsoid ($4/3\pi abc$) using the length (a), width (b), and perceived height (c) measurements. This formula will somewhat overestimate volume for those endocarps with a central intrusion (e.g. *Solenotinus* or *Dentata*). However, given that endocarp shape is consistent within each major *Viburnum* clade, possible implications of this overestimate can be evaluated on a clade by clade basis.

Elliptical Fourier Analysis of Endocarp Shape—To facilitate phylogenetic studies, we analyzed endocarp shape using elliptical Fourier analysis (EFA) as opposed to landmark or sliding-landmark approaches (Jacques and Zhou 2010); this allowed us to circumvent the lack of reliable, homologous landmarks (Wefferling et al. 2013). Using Adobe Photoshop CC 2014.2.1, digital images of individual endocarp cross sections were cropped and binarized such that the endocarp cross section was completely filled in using the smart selection tool, and the background was deleted to produce a black and white image.

EFA was performed using the Momocs package (Bonhomme et al. 2014) in R (R Core Team 2019) with the binarized images. The 50 samples for each of the four focal species for the intraspecific study (*V. acerifolium*,

V. dentatum, *V. dilatatum*, and *V. prunifolium*) were analyzed separately to determine the extent of variation within a species. Then, EFA, as described below, was performed on the dataset including 122 species of *Viburnum*.

Within Momocs, the direction argument belonging to the `coo_slidedirection` function was set to north by default in the initial stages of scaling the images. At the start of the scaling step, Momocs would begin by placing the landmark in the center of the image and moving north until reaching the upper limit of the endocarp (e.g. dorsal side). Particularly in *Solenotinus*, where endocarps are horseshoe-like in shape, the initial landmark was often placed in a position in the image outside of the endocarp itself, below the ventral side of the endocarp. As the landmark moved north it would reach the lower limit (ventral side) rather than the upper limit (dorsal side) as it did on all other endocarp images. In these instances, the image of the endocarp would be inverted and cause the generation of a morphospace that included biologically impossible shapes. To correct for this problem, we resized and cropped the image of horseshoe shaped endocarps to ensure that the first landmark would land on the seed itself between the dorsal and ventral limits of the endocarp. The data were then used in a principal component analysis (PCA) using Momocs `efourier` function in R (R Core Team 2019).

Phylogenetic Analyses—We assembled a data matrix for 115 *Viburnum* species including 10 gene regions (nrITS and nine plastid regions: *matK*, *ndhF*, *petB-petD*, *rbcL*, *rpl32-trnL*^(UAG), *trnC-ycf6*, *trnH-psbA*, *trnK*, and *trnS-trnG*) obtained from the data used in reconstructing the most comprehensive *Viburnum* phylogeny published to date (Landis et al. 2020; Appendix 1). Gene regions were aligned individually using Muscle v. 3.8.31 (Edgar 2004). Partitionfinder v. 2.1.1 (Lanfear et al. 2012) was used to determine the best partitioning strategy for the 10 gene regions and corresponding best fit models of sequence evolution. For this cpDNA + nrITS-based analysis, *V. clemensiae* was used to root the tree based on prior studies using *Sambucus* L. species as outgroups (Donoghue et al. 2004; Winkworth and Donoghue 2005; Clement and Donoghue 2011; but see Lens et al. 2016).

Phylogenetic analyses were conducted in both a maximum likelihood (ML) and a Bayesian inference framework (BI). ML analyses were performed in Garli v. 2.0 (Zwickl 2006). ML analyses were repeated independently five times with each analysis iterated five times to ensure that likelihood scores were similar among runs. Additionally, ML bootstrap analyses with 500 replicates were performed using the same models of sequence evolution. BI analyses were run in MrBayes v. 3.2.6 (Huelsenbeck and Ronquist 2001; Ronquist and Huelsenbeck 2003) for 40 million generations with four chains and model parameters among partitions unlinked. The posterior distribution was sampled every 1000 generations, and the convergence and burn-in were determined visually by inspecting plots of all parameters in Tracer v. 1.7 (Rambaut et al. 2018). The burn-in was removed prior to summarizing model parameters and sampling trees from the posterior distribution.

Analyses of endocarp evolution were also conducted on the maximum clade credibility tree topology of Landis et al. (2020) based on RADseq data, which was pruned to include just the 115 species in our cpDNA + nrITS dataset.

Morphological Evolution—Continuous trait data pertaining to endocarp shape measurements obtained from the EFA, as well as volume estimations, were reconstructed on the 115-species tree with branch lengths based on the 10-gene cpDNA + nrITS data matrix (Landis et al. 2020). Ancestral character state analysis under ML was performed and visualized using the fastAnc function of the phytools package (Revell 2012) in R (R Core Team 2019). Using the RADseq tree without branch lengths (Landis et al. 2020), we reconstructed ancestral character states for the same traits under maximum parsimony in Mesquite v. 3.51 (Maddison and Maddison 2019).

A phylomorphospace was generated using APE (Paradis et al. 2004) and phytools (Revell 2012) packages in R (R Core Team 2019) using the 115-species *Viburnum* phylogeny reconstructed from the 10-gene data set and the morphospace generated from PC1 and PC2 from the EFA. Internal nodes were placed based on ancestral character state analysis using fastAnc on the first and second principal component scores.

Quantifying Parallel Evolution—Having measured endocarp shape as a continuous trait, we were able to apply a tree-based approach to quantifying putative cases of parallel evolution that uses both phenotypic distances and the tree topology (Stayton 2015). For any two taxa hypothesized to have evolved in parallel, the inferred evolution through phenotypic space is likely to diverge before converging on a similar part of the phylomorphospace. To this end, using the metrics proposed by Stayton (2015), we calculated a convergence index, C1, that measures the amount of convergent evolution that has occurred based on the contemporary phenotypic distance between two selected species (i.e. the Euclidean distance between them in the phylomorphospace, D_{Hip}) and the maximum distance attained anywhere along the branches that trace back to their most recent common

ancestor (D_{\max}). This metric ranges from 0 to 1, with C1 approaching 1 when the two taxa being compared have evolved very similar endocarp shapes from very different parts of the phylomorphospace (Stayton 2015).

To explore parallel evolution of endocarp shape in light of phylogeny in *Viburnum*, we applied the C1 metric to three potential cases of parallel evolution based on generalized endocarp shapes that occur in more than one *Viburnum* clade: 1) compressed, non-undulating endocarps (e.g. *Opulus* and *Lentago*), 2) round endocarps with a prominent central intrusion (e.g. *Solenotinus*, *Dentata*, and *Oreinotinus* of northern Mexico), and 3) round endocarps with a very reduced central intrusion (including *V. clemensiae*, *Tinus*, and *Oreinotinus* of South America). We calculated C1 for all pairwise combinations among members of the putatively convergent clades using the `convrat` function in the `convevol` package (Stayton 2015) in R (R Core Team 2019) and averaged the results. Significance was assessed using the `convratsig` function in `convevol` (Stayton 2015) with 100 simulations.

RESULTS

Intraspecific Variation of *Viburnum* Endocarps—We found relatively little variation within the four species sampled (Fig. S1). However, our samples of *V. dentatum* did show differences on the ventral and dorsal sides of the endocarp due to irregularities associated with grooving (Fig. S1).

Diversity of *Viburnum* Endocarps—We examined the distribution of endocarp form across *Viburnum* by plotting endocarp length against the ratio of width to perceived height (W:PH; Fig. 2). This showed that endocarp length varied widely within clades, but that most clades fell into clusters along the W:PH axis (Fig. 2). First, *Oreinodentinus* (*Oreinotinus* + *Dentata*), *Tinus*, *V. clemensiae*, and many species of *Solenotinus* have more or less spherical endocarp shapes in cross section (W:PH = 1–1.5), with little to no dorsal-ventral compression. At the other end of the W:PH spectrum are most species of *Lentago*, *Lobata*, *Opulus*, *Punctata*, and *Urceolata*, with distinctly flattened endocarps in cross section (W:PH of 2.5–4). The region in between these two extremes (W:PH of 1.5–2.5) contains the remaining *Viburnum* clades. Endocarps in this zone generally show some degree of dorsal-ventral compression with usually two dorsal and three ventral undulations roughly forming the shape of a “bat-silhouette.” Although most clades are mainly confined to one of these three W:PH zones, *Solenotinus*, *Sambucina*, and *Lutescentia*, are more diverse and span two or all three of the zones. We also noted the absence of species with endocarps that are round and long (upper left quadrant of the morphospace) or flattened and short (lower right quadrant) (Fig. 2).

The PCA of the elliptical Fourier analysis of endocarp shape recovered 49.5% of the variation in the first principal component (PC) and 21.5% of the variation in the PC2 (Fig. S2). The morphospace created by PC1 and PC2 reflects the degree of curvature of the lateral “arms” of the endocarp around a ventral groove along PC1 and the degree of compression of the endocarp along PC2. As PC1 increases, the lateral arms of the endocarp shift from being curved around the ventral groove (creating a horseshoe shape) to uncurved (lacking a ventral groove). As values for PC2 increase, endocarps shift from more compressed to rounded.

Endocarp volume ranged from 0.9 cm³ to 2.65 cm³ with a mean of 0.59 cm³ (\pm 0.39 cm³) and a median of 0.51 cm³ (Table S1). Although for most species we have made measurements of only one or two endocarps, we note that our findings are consistent with descriptions and measurements of endocarp/seed sizes in the literature (e.g. Kern 1951; Donoghue 1983b; Hara 1983; Jacobs et al. 2008; Yang and Malécot 2011). Not surprisingly, clades containing many species (and with

many species in our sample) show the greatest variation in endocarp volume. *Oreinotinus*, with 22 species in our sample, has a median size of 0.43 cm³, but endocarps in this clade range from 0.20–2.65 cm³, a difference of some 13-fold. Likewise, *Succotinus*, with 19 species in our sample, has a median endocarp volume of 0.37 cm³, but ranges from 0.09–1.10 cm³, for a 12-fold difference.

Although endocarp volume does vary considerably within clades (Table S1), we also note that volume does still broadly reflect phylogenetic relationships (Figs. S3, S4). We are struck, for example, that the *Laminotinus* clade has generally small endocarp volumes, with median values of 0.37 cm³ in *Succotinus*, 0.35 cm³ in *Lobata*, and 0.36 cm³ in *Coriacea*. This contrasts with generally larger volumes in *Valvatotinus*, with median values of 0.78 cm³ in *Punctata*, 0.77 cm³ in *Lentago*, and 0.66 cm³ in *Euviburnum*. *Oreinodentinus* shows intermediate values, with median values of 0.50 cm³ in *Dentata* and 0.43 cm³ in *Oreinotinus*.

Evolution of *Viburnum* Endocarps—The *Viburnum* phylogeny recovered here from our cpDNA + nrITS dataset is congruent with prior analyses based on these data (Fig. 3). Using this tree as well as the RAD-seq tree, we conducted ancestral character state analyses of W:PH, as this was the variable that best separated endocarp shapes (Fig. 3; Fig. S5). In the cpDNA + nrITS tree, the ancestor of *Regulaviburnum* was inferred to have had somewhat compressed endocarps with dorsal and ventral grooving (green in Fig. 3). Shifts to rounder endocarps (red and orange in Fig. 3) were seen in *V. clemensiae* and several clades (*Tinus*, *Oreinotinus*, and *Solenotinus*), while shifts to highly compressed endocarps (blue in Fig. 3) were especially evident in *Opulus* and *Lentago*. These derivative shapes also greatly reduce or lose the dorsal and ventral grooving. Despite topological differences in the RAD-seq tree, shifts from compressed endocarps with grooving to rounder and to highly compressed endocarps without grooving were identified in the same clades (Fig. S5).

Visualizing the tree in the morphospace (Fig. 4) confirmed that the majority of *Viburnum* clades occupied a part of the morphospace represented by the symplesiomorphic moderately compressed and grooved endocarp form. From there, several lineages independently explored different pathways to the round condition (lower PC1 scores) while also obtaining a wide range of lengths (PC2 in Fig. 4). On the PC2 axis, increasing PC2 scores included endocarps that appeared roughly round in cross section but had a large ventral intrusion or groove, with downward curving lateral arms. The PCA (Fig. 4; Fig. S2) did not as strongly separate highly compressed endocarps (in the upper right quadrant) with greatly reduced grooving as compared to other data visualization approaches (Figs. 2, 3).

Taken together, these analyses identified three instances of parallel evolution (Figs. 3, 4), which we further investigated using a statistical approach (Table 1; Fig. 5). The first major case of parallel evolution was of round shapes with limited grooving and little central intrusion, as seen in the *Oreinotinus* species of South America as well as *Tinus* and *V. clemensiae*. These species shared a low W:PH ratio (Fig. 2) and occupied an area of the phylomorphospace that was distinct from that of the ancestral endocarp shape (Fig. 4). To visualize the C1 calculation, we traced the branches leading to *V. tinus* L. (*Tinus*) and to *V. tinoides* L.f. (*Oreinotinus*) from their most recent common ancestor to the modern shapes through the morphospace to highlight maximum (D_{\max}) and contemporary (D_{tip})

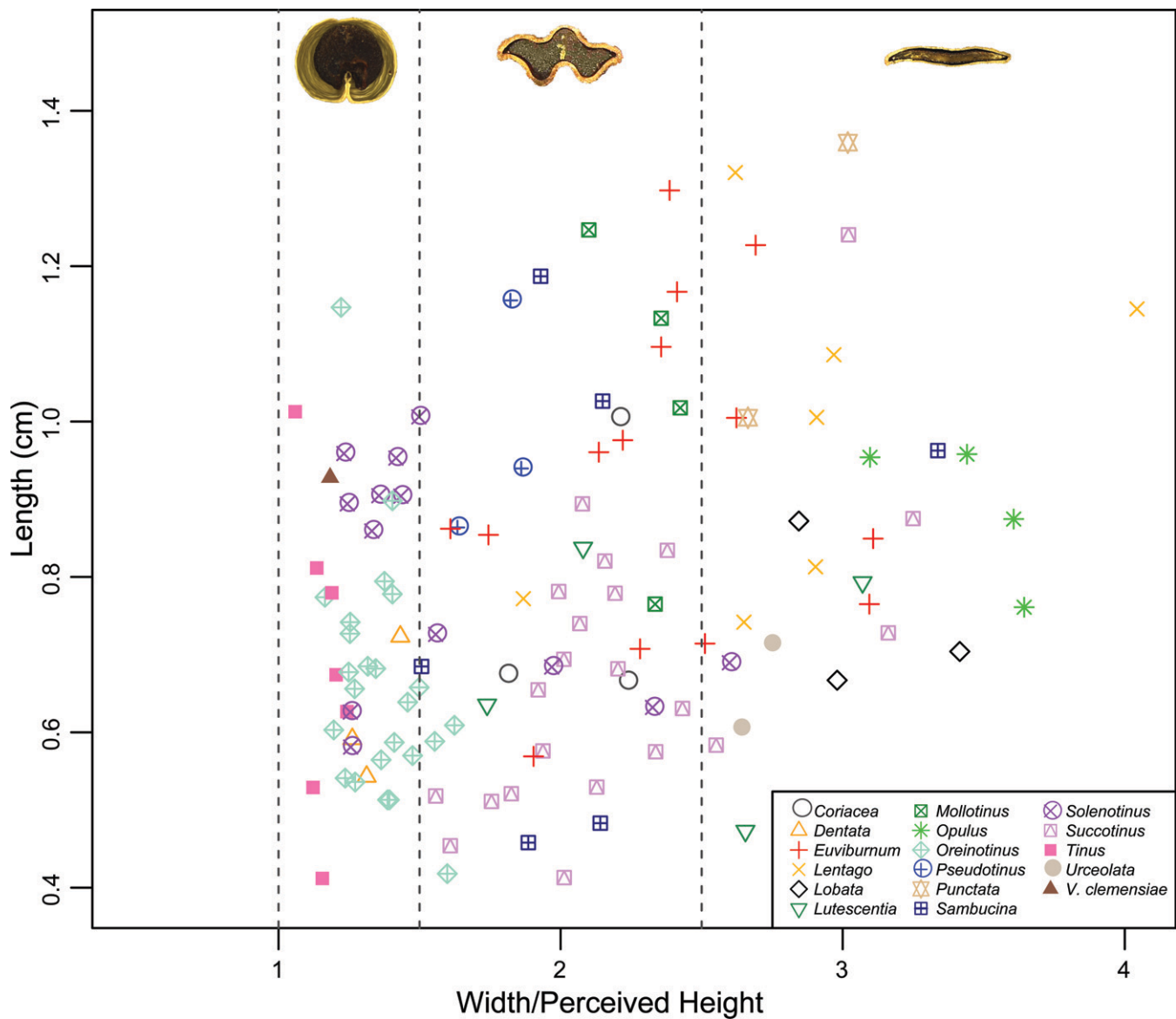


FIG. 2. Scatterplot showing the width/perceived height ratio on the X axis and absolute length on the Y axis ($n = 122$). Clades are denoted by color and symbol. Exemplar endocarps along the top show how an increase in the W:PH ratio corresponds to dorsal-ventral compression. Vertical dotted lines demarcate three regions of the morphospace that broadly correspond with endocarp form. Note that while lengths are variable within clades, *Tinus*, *Oreinotinus*, *Dentata*, *Solenotinus*, and *V. clemensiae* generally fall below a W:PH of 1.5, whereas *Lentago*, *Opulus*, *Punctata*, and *Lobata* fall above 2.5.

phenotypic distances (Fig. 5). The C1 values for this comparison and the majority of comparisons among the species of *Tinus*, South American *Oreinotinus*, and *V. clemensiae* demonstrated that these endocarps had evolved to be more similar than would have been expected by chance ($p < 0.05$; Table 1; Fig. 5), supporting our hypothesis that this endocarp form evolved in parallel in these three groups.

While *Tinus*, some *Oreinotinus*, and *V. clemensiae* have round endocarps virtually lacking a ventral intrusion (low PC1 and PC2 values; Fig. 4), most *Solenotinus* species are round in cross section but with a prominent ventral intrusion. Similar forms exist among the variable round endocarps of *Oreinotinus* (Fig. 3). In particular, *Dentata* species have endocarps with a conspicuous ventral intrusion as do species of *Oreinotinus* from northern Mexico. We focused our statistical comparisons on *V. foetens* Decne. (*Solenotinus*), *V. dentatum* (*Dentata*), *V. loeseneri* Graebn., and *V. microcarpum* Schltdl. & Cham. (*Oreinotinus* species of northern Mexico). All of these comparisons

yield significant C1 values ($p < 0.05$; Table 1; Fig. 5). Additional comparisons of species of *Solenotinus*, *Dentata*, and Mexican *Oreinotinus* species resulted in about half of these comparisons yielding significant C1 values ($p < 0.05$; Table 1; Fig. 5). These results support our hypothesis that rounded endocarps with a central intrusion have evolved in parallel in these clades.

The final endocarp form hypothesized to have evolved in parallel was compressed endocarps with little or no grooving, primarily observed in the *Opulus* and *Lentago* clades. We focused on comparing *V. lentago* L. (*Lentago*) and three species of the *Opulus* clade (*V. edule* (Michx.) Raf., *V. opulus* L., and *V. trilobum* Marshall), all of which yielded significant C1 values ($p < 0.05$; Table 1; Fig. 5). Nearly half of the comparisons between species of the *Lentago* and *Opulus* clades were more similar than expected by chance ($p < 0.05$; Table 1; Fig. 5). Additionally, species in two other clades, *V. schensianum* Maxim. of *Euviburnum* and *V. chingii* P.S.Hsu of *Solenotinus*, were seen to occupy the same region of the phylomorphospace as the

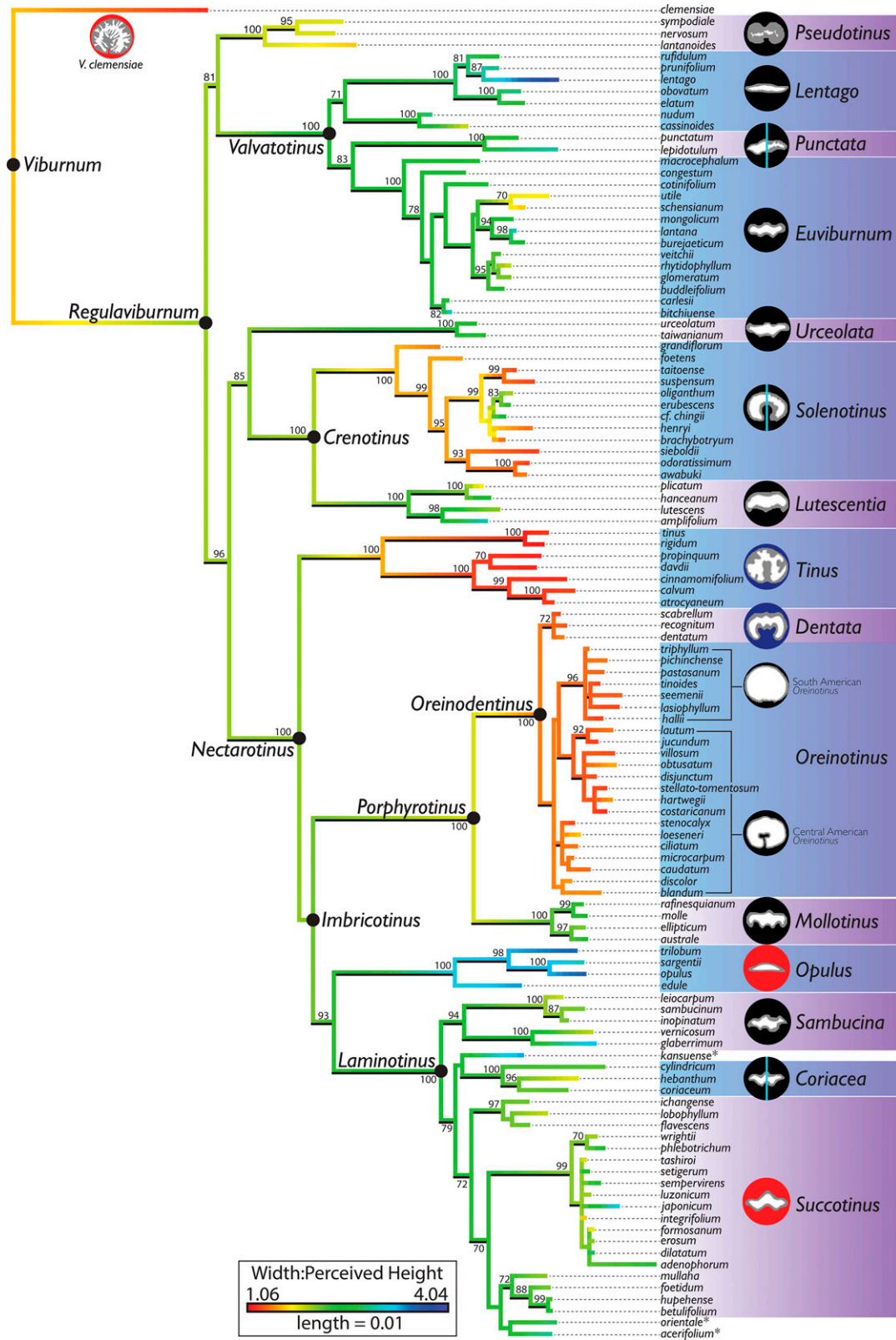


FIG. 3. Maximum clade credibility tree from the Bayesian analysis of cpDNA + nrITS data for 115 species of *Viburnum*, showing inferred ancestral Width:Perceived Height (W:PH) values. Posterior probabilities > 0.95 are indicated by black lines subtending branches and maximum likelihood bootstrap values > 70 are placed above or below the branches. Named clades of *Viburnum* (Clement et al. 2014) are indicated with a black dot adjacent to a node or to the right of the taxon names; members of Lobata (a clade recovered in RAD-seq analyses: Landis et al. 2020) do not form a clade here and are marked with an asterisk. Fruit cross sections reflect the fruit and endocarp characters indicative of that group. Fruit cross sections show fruit color, endocarp shape, the relative amount of pulp, and ruminant endosperm. For clades with more than one endocarp form, either two separate fruit cross sections are shown (e.g. Oreinotinus), or a single cross section is shown with a blue line separating the two possible endocarp shapes on the left and right-hand sides of the fruit (e.g. Punctata, Solenotinus, and Coriacea).

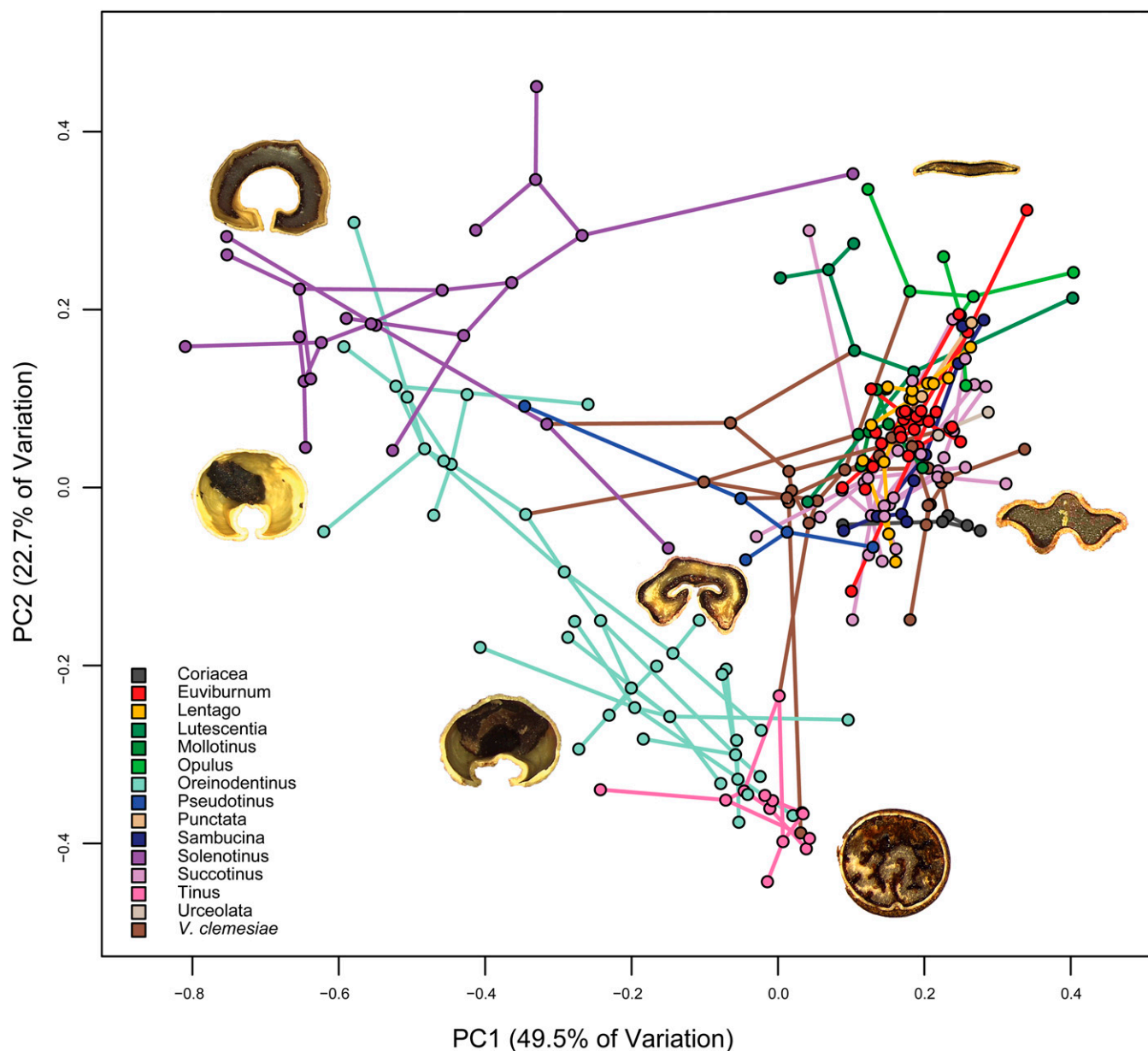


FIG. 4. Phylomorphospace based on the first two principal components from the Elliptical Fourier Analysis, showing *Viburnum* phylogeny based on nine plastid gene regions and nrITS ($n = 115$). Colors of the branches denote major *Viburnum* clades (Fig. 3). Representative endocarp images have been positioned to illustrate how shape varies across the morphospace.

majority of *Opulus* and *Lentago* species (Fig. 4). These species were also supported as having evolved this endocarp shape in parallel ($p < 0.05$; Table 1; Fig. 5).

DISCUSSION

Endocarp Morphology and Taxonomy—Endocarp shape has long been considered a diagnostic feature within *Viburnum* and is especially useful in distinguishing the traditional sections from one another (Oersted 1861; Rehder 1940; Hara 1983). Our analyses confirm that most of the major clades are distinguishable on this basis (Figs. 2, 4, 6). For instance, all species of the *Tinus* clade have rounded endocarps with a highly reduced ventral intrusion in cross section (Fig. 6D), while species of the *Lentago* clade have highly compressed endocarps with little grooving (Fig. 6A). Our analyses also recover

distinctive shapes for several clades that have only recently been recognized; for example, the *Punctata*, *Lutescentia*, *Sambucina*, and *Coriacea* clades of the former *Viburnum* section *Megalotinus* (Maxim.) Rehder (Clement and Donoghue 2011; Clement et al. 2014; Figs. 3, 6A).

Importantly, characteristic endocarp shapes have been retained within the major clades despite considerable variation in endocarp/seed size within these clades (Fig. 2; Table S1; Figs. S3, S4). In addition to the broad phylogenetic patterns in endocarp volume highlighted above, we note that there are evolutionary patterns in endocarp size within some clades. In *Oreinotinus*, the aptly named *V. microcarpum* has an endocarp volume of 0.21 cm^3 , and similarly small sizes are found in its eastern and central Mexican relatives (e.g. *V. caudatum* Greenm., 0.23 cm^3 ; *V. loeseneri*, 0.32 cm^3). In contrast, the nine species in our sample of the South American *Oreinotinus* clade

TABLE 1. Measurements of convergence following Stayton (2015). Categories of endocarp shape hypothesized to have evolved in parallel include round endocarps with and without a central intrusion and compressed endocarps without grooving. For each comparison of a pair of species, C1 and a corresponding p value are reported. For clade-level comparisons, average C1 and p values are reported, representing all possible pairwise species comparisons between clades. Additionally, we report the proportion of such pairwise comparisons that are significant. Northern Mexican Oreinotinus are *V. caudatum*, *V. ciliatum*, *V. loeseneri*, *V. microcarpum*, and *V. stenocalyx*. Figure 5 shows the location in the phylomorphospace of the species and clades examined here.

	C1	p	Proportion significant
Round without central intrusion			
<i>V. clemensiae</i> + <i>V. tinus</i>	0.9638	0.0000	–
<i>V. clemensiae</i> + Tinus	0.8826	0.0198	6/7
<i>V. clemensiae</i> + <i>V. tinoides</i>	0.8635	0.0000	–
<i>V. clemensiae</i> + S.A. Oreinotinus	0.7620	0.0156	7/7
<i>V. tinus</i> + <i>V. tinoides</i>	0.8266	0.0000	–
Tinus + S.A. Oreinotinus	0.7490	0.0337	35/49
Round with central intrusion			
<i>V. dentatum</i> + <i>V. microcarpum</i>	0.7195	0.0396	–
<i>V. dentatum</i> + <i>V. loeseneri</i>	0.5713	0.0594	–
Dentata + N. Mexican Oreinotinus	0.6919	0.0462	8/15
<i>V. foetens</i> + <i>V. microcarpum</i>	0.7060	0.0396	–
<i>V. foetens</i> + <i>V. loeseneri</i>	0.7463	0.0396	–
Solenotinus + N. Mexican Oreinotinus	0.5834	0.1616	30/60
<i>V. dentatum</i> + <i>V. foetens</i>	0.4577	0.1188	–
Dentata + Solenotinus	0.5984	0.1356	18/36
Compressed without grooving			
<i>V. opulus</i> + <i>V. lentago</i>	0.6840	0.0297	–
<i>V. trilobum</i> + <i>V. lentago</i>	0.7572	0.0297	–
<i>V. edule</i> + <i>V. lentago</i>	0.2326	0.3465	–
Opulus + Lentago	0.5850	0.0902	13/28
<i>V. schensianum</i> + <i>V. opulus</i>	0.8394	0.0000	–
<i>V. schensianum</i> + <i>V. lentago</i>	0.7718	0.0198	–
<i>V. schensianum</i> + <i>V. chingii</i>	0.7042	0.0198	–
<i>V. chingii</i> + <i>V. opulus</i>	0.8119	0.0198	–
<i>V. chingii</i> + <i>V. lentago</i>	0.6784	0.0198	–

have much larger endocarps, averaging 0.81 cm^3 . This difference in overall endocarp volume corresponds with a change in shape. As Oreinotinus spread from North to South America (Landis et al. 2020), the ventral intrusion was reduced. Other noteworthy cases of endocarp size variation within clades include the relatively large sizes of the Chinese *V. setigerum* Hance (1.10 cm^3) and its Japanese sister species, *V. phlebotrimum* Siebold & Zucc. (0.63 cm^3) within Succotinus (where the median endocarp volume is 0.37 cm^3). In the Lentago clade, *V. cassinoides* L. (0.34 cm^3) and *V. nudum* L. (0.42 cm^3) have much smaller endocarps than members of their sister clade, especially *V. rufidulum* Raf. (1.35 cm^3) and *V. prunifolium* (1.37 cm^3).

Parallel Evolution of Viburnum Fruit Syndromes—Beyond confirming the taxonomic value of sometimes rather subtle differences in endocarp shape, our phylogenetic analyses allowed us to trace the paths of endocarp evolution. We examined such patterns using two tree topologies, the first based on cpDNA + nrITS data (Fig. 3) and the second based largely on RAD-seq data (Landis et al. 2020; Fig. S5). We have featured the cpDNA + nrITS tree in Fig. 3 in order to highlight our latest analysis of this expanding dataset, but all of our basic conclusions regarding the evolution of endocarp shapes are supported on both trees (see below and Fig. S5).

The endocarps of the first viburnums were likely moderately compressed, with two shallow dorsal grooves and three shallow ventral grooves (cf. Jacobs et al. 2008). Endocarps of this form are featured in Fig. 6A, with arrows marking the grooves as seen in a cross section of *V. buddleifolium* C.H. Wright of the Euviburnum clade. This basic form was retained in multiple clades, though with slight but consistent differences in shape and size (Fig. 6A). From this starting point there appear to have been several parallel shifts in endocarp form. Highly

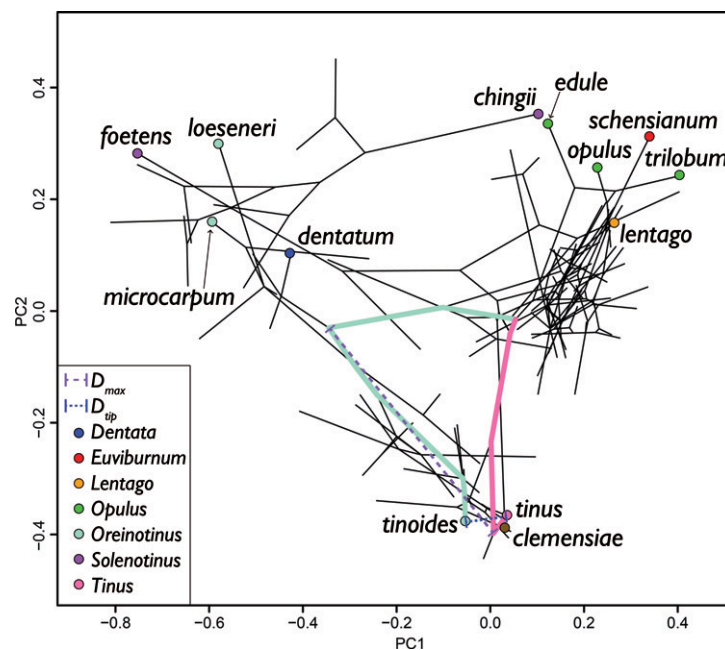


FIG. 5. Phylomorphospace highlighting species used in calculating C1 values and statistical significance (Stayton 2015). Highlighted are the branches connecting two focal taxa, *V. tinoides* (Oreinotinus) and *V. tinus* (Tinus), that independently evolved round endocarps without a central intrusion independently. D_{\max} is the maximum Euclidian distance (dashed line) separating the branches leading to *V. tinoides* from the branches leading to *V. tinus*; D_{tip} is the Euclidean distances (dotted line) between the modern endocarp forms of *V. tinoides* and *V. tinus*. For any two species being compared, $C1 = 1 - (D_{\text{tip}}/D_{\max})$. All taxa highlighted in pairwise species comparisons in Table 1 are labeled and colored by clade.

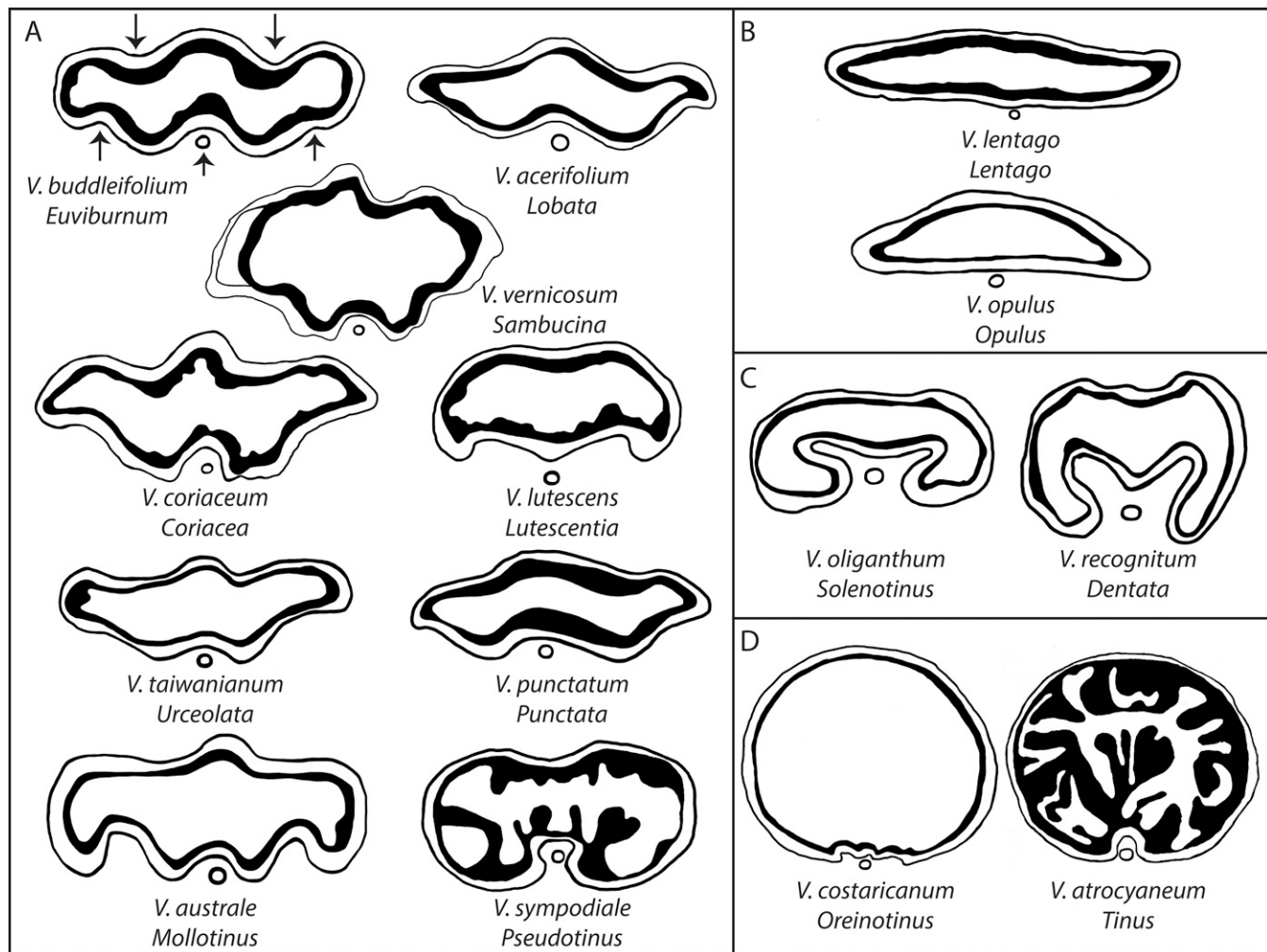


FIG. 6. Representative endocarp shapes for each major *Viburnum* clade. Endocarp cross sections are from camera lucida drawings of endocarps obtained from herbarium specimens. The outermost white area represents the endocarp and the inner black area represents the seed coat (testa). The black seed coat can be variously thickened (e.g. *V. lutescens*) or show more complex patterns of rumination extending into the endosperm (e.g. *V. atrocyaneum*). The small circle underneath each endocarp form represents the central vascular bundle that runs along the ventral axis of the ovary. A. Endocarp shapes more or less corresponding with an inferred ancestral endocarp that is compressed and grooved. Arrows associated with *V. buddleifolium* indicate the two dorsal and three ventral grooves characteristic of this ancestral endocarp form. B–D. Derived endocarp forms. B. Parallel evolution of compressed endocarps without grooving. C. Parallel evolution of round endocarps with a central intrusion. D. Parallel evolution of round endocarps with a very reduced central intrusion.

compressed and more or less grooveless endocarps evolved independently, most notably in the *Opulus* and *Lentago* clades (Fig. 6B). Rounded endocarps evolved separately in the *Tinus* and *Oreinodontinus* clades, in some members of the *Solenotinus* clade, and in *V. clemensiae*. More specifically, rounded but horseshoe-shaped endocarps (i.e. with a prominent ventral intrusion), characterize the *Dentata* clade in eastern North America, several species of *Oreinotinus* in northern Mexico, and some *Solenotinus* in Asia (Fig. 6C). The ventral groove is almost completely absent in *Tinus* species in Eurasia, in the species of *Oreinotinus* from southern Mexico to South America, and in *V. clemensiae* of Borneo (Fig. 6D). These changes appear to have been unidirectional; that is, we have inferred no reversals from the several derived endocarp forms back to a more ancestral form.

We are also able to assess how changes in endocarp shape have been related to changes in other fruit traits: color development pattern (sequential versus synchronous, Fig. 1F–G), mature fruit color, and, for some species, the volume, moisture, lipid, and sugar content of the mesocarp (Sinnott-Armstrong

et al. 2020). Sinnott-Armstrong et al. (2020) focused special attention on two derived “fruit syndromes” within *Viburnum*, both of which evolved several times. In one of these syndromes, flattened endocarps are associated with red color, and with ample watery mesocarp tissue, rich in carbohydrates. In the other, rounded endocarps are associated with blue color, and with a thin mealy-textured mesocarp, rich in lipids. Our results are fully consistent with the recognition of these two syndromes, but here we recognize other trait combinations that involve fewer fruit variables and occur only occasionally. Such combinations of traits have arisen in several different ways. In some cases, the inferred ancestral endocarp shape has been retained in a lineage that has subsequently evolved a different color, mesocarp type, and/or nutritional content. For example, *Mollotinus* species appear to have maintained the ancestral endocarp shape (Figs. 3, 4, 6A), but they differ from inferred ancestral fruits in undergoing synchronous color development and in having higher lipid content (Sinnott-Armstrong et al. 2020). Other combinations have come about as endocarp shape has evolved within clades that have otherwise

retained ancestral fruit traits. For example, species in the Solenotinus clade appear to have retained sequential color maturation, intermediate pulp volume, and low lipid content, yet within this clade a number of different endocarp shapes have evolved, including derived horseshoe-shaped forms (Figs. 3, 4, 6C).

In yet other cases, several fruit traits appear to have evolved along the same branch in the tree, and this has yielded several evolutionarily one-off fruit types. The best example is *V. clemensiae*. Although some uncertainty remains about the exact phylogenetic placement of this species (Landis et al. 2020), it is clear that it represents a very early and long branch in the *Viburnum* tree. It appears to have evolved a rounded endocarp, but with red color at maturity, a reduced mealy mesocarp, and a peculiar form of ruminant endosperm (Jacobs et al. 2008; Clement et al. 2014). As this combination evolved nowhere else in *Viburnum*, it was not flagged as a syndrome by Sinnott-Armstrong et al. (2020). But, cases like this show us that elements of the syndromes of Sinnott-Armstrong et al. (2020) do not strictly co-occur. Round endocarps are associated with several other traits in the blue syndrome of Sinnott-Armstrong et al. (2020), and, likewise, flattened endocarps are characteristic of the red syndrome. However, these derived endocarp shapes are not limited to these two syndromes. In fact, some of the most extreme cases of parallel evolution of a particular derived endocarp shape (Fig. 5; Table 1) appear in the context of otherwise highly divergent fruits. An excellent example of such parallelism is the evolution of similar rounded endocarps in *V. clemensiae* on the one hand, and in the Tinus clade on the other hand. The same is also true of highly flattened endocarps. These are found in the *Opulus* clade, in which the fruits are red and juicy (hence the red syndrome), but they also evolved in the Lentago clade in the context of sequential color development, black color at maturity, and mealy texture.

On the Evolution of 'Fruit Syndromes'—What do these observations tell us about fruit evolution? The appearance of very similar endocarp shapes in different fruit backgrounds assures us that these traits can indeed evolve independently of one another. It also shows that there is a wider range of functional configurations than the several syndromes recognized by Sinnott-Armstrong et al. (2020) may suggest. The one-off fruits of *V. clemensiae* demonstrate that round endocarps need not be associated with the blue syndrome, and, therefore, that there are likely other factors driving endocarp shape. What these factors are is unclear. A particular endocarp shape may evolve to maximize dispersal by particular resident or migratory birds, but endocarp shape relates to other functions such as seed germination, and the combinations of fruit traits that we observe presumably represent trade-offs with respect to these various functions. Such trade-offs extend to other features that we have not focused on here, perhaps especially seed coat traits, including the production of ruminant endosperm in a number of clades. Notably, although the round endocarps of Tinus, Oreinotinus, and *V. clemensiae* have evolved in parallel, they have diverged significantly in several other seed traits (Jacobs et al. 2008). Tinus and *V. clemensiae* have well-developed ruminant endosperm, but of different developmental types (Type 2A in *V. clemensiae* and Type 2B in Tinus; Jacobs et al. 2008), whereas ruminant endosperm is absent or very limited in Oreinotinus (Fig. 6D). Likewise, there are marked differences in endocarp and seed coat thickness and cell structure, some of which are highly consistent with phylogeny. For example, thinner seed coats of cuboidal or

rectangular cells appear to mark the entire Nectarotinus clade, while the rest of the species have retained a thicker testa with palisade-shaped cells (cf. Jacobs et al. 2008).

Even more generally, how do these observations bear on the concept of syndromes? In reflecting on fruit syndromes, a comparison to the familiar pollination syndromes is useful. We recognize a certain combination of flower traits as the hummingbird pollination syndrome: long tubular red-colored corollas that open during the day and produce copious nectar and little scent. This combination has emerged repeatedly, in distantly related angiosperm lineages in relation to selection by hummingbirds, with their particular perceptual abilities (e.g. Abrahamczyk and Renner 2015). But, it is clear that the individual elements of the hummingbird syndrome have evolved elsewhere, sometimes in relation to other pollinators. For example, long tubular corollas have also evolved in connection with hawkmoth pollination, where the flowers are typically white, scented, and open at night. Observations such as this do not diminish the value of recognizing syndromes, but they do serve to highlight that particular traits of interest can evolve independently of the traits with which they are most often associated, and that they can potentially function in connection with multiple syndromes or fall completely outside of commonly described syndromes (Ollerton et al. 2009; Rosas-Guerrero et al. 2014). They also highlight that a given trait can influence a variety of functions at once. A long corolla tube might attract particular pollinators, but could also keep out unwanted visitors. Nevertheless, it is important to note that particular traits, such as tubular corollas, do not evolve in connection with every pollination syndrome (e.g. with beetle or wind pollination).

All of these observations apply to the traits that constitute fruit syndromes, and we note, in particular, that not all species fall within proposed syndromes, nor do we observe every possible combination of fruit traits in *Viburnum* or more generally (cf. Beaulieu and Donoghue 2013). For example, we do not find flattened endocarps with scant lipid-rich flesh and blue color, or round endocarps embedded in a copious watery mesocarp. This implies that such combinations are either not evolutionarily accessible, or that they have not evolved because they would function poorly. Compared to the traits associated with pollination syndromes, we still know very little about the function of most fruit traits (except in the broadest terms; e.g. fleshy fruits are selected by birds). Nevertheless, speculation on function can be useful in framing potential tests. For example, we might hypothesize that large endocarps surrounded by a thin layer of watery mesocarp are not found because in order for birds to assume the costs associated with ingesting a large endocarp, fruits need to provide sufficient nutritional benefit; for example, by providing either a large amount of flesh or flesh rich in lipids.

CONCLUSIONS

The colorful drupe fruits of *Viburnum* hide a wide array of endocarp shapes within. The sometimes subtle variation in endocarp shape can be difficult to describe, but our morphometric and phylogenetic analyses demonstrate that endocarp shapes are largely consistent within and among species. Also, different shapes distinguish many of the major clades within *Viburnum* despite considerable variation in absolute size. Our quantitative analyses provide statistical support for several cases of parallel evolution from a moderately flattened and

grooved ancestral form toward rounded forms and ungrooved flattened forms. In some cases, these shifts are tightly correlated with changes in the color and nutritional content of the pulp, which supports the recognition of derived fruit “syndromes” that have evolved several times independently and may relate to dispersal primarily by resident versus migrant birds (Sinnott-Armstrong et al. 2020). However, our expanded analyses, focused specifically on endocarp form, highlight that parallel evolution in endocarp shape sometimes occurs in drupes that are otherwise highly dissimilar. While this confirms that these fruit traits can vary quite independently, it also demonstrates the existence of an even wider variety of strategies with respect to dispersal and/or germination. Our results set the stage for understanding the integrated evolution of an entire set of fruit and seed traits in relation to the several vital functions that they carry out.

ACKNOWLEDGMENTS

We thank S. Barish for assistance with data collection, E. L. Spriggs for help with data analysis, P. W. Sweeney for collecting viburnums in the field, and M. Van Clef for permission to collect in Nayfield Preserve. We are grateful to Miranda Sinnott-Armstrong for her careful reading and insights, and to the Erika Edwards lab group at Yale University for helpful discussion. Our thanks also to Tao Chen and the Xianhu Botanical Garden, and Hang Sun, Tao Deng, and Yongsheng Chen, and the Kunming Botanical Institute for facilitating and assisting with fieldwork in China. Additionally, we are grateful to Michael Dossman and the Arnold Arboretum, and Anthony Brach and the Harvard University Herbaria, for access to and assistance with the *Viburnum* collections. The authors acknowledge use of the ELSA high performance computing cluster at The College of New Jersey for conducting the research reported in this paper. This cluster is funded by the National Science Foundation under grant number OAC-1828163. This work was funded by the Biology Department and School of Science at The College of New Jersey, and a National Science Foundation grant (DEB-1145606) to M. J. Donoghue, W. L. Clement, and P. W. Sweeney.

AUTHOR CONTRIBUTIONS

WLC and MJD designed the research project, AG and PG collected sequence data and conducted phylogenetic analyses, TJS photographed and collected endocarp morphology data, TJS and WLC conducted analyses, and WLC and MJD drafted the paper.

LITERATURE CITED

- Abrahamczyk, S. and S. S. Renner. 2015. The temporal build-up of hummingbird/plant mutualisms in North America and temperate South America. *BMC Evolutionary Biology* 15: 104.
- Abramoff, M. D., P. J. Magalhaes, and S. J. Ram. 2004. Image processing with ImageJ. *Biophotonics International* 11: 36–42.
- Beaulieu, J. M. and M. J. Donoghue. 2013. Fruit evolution and diversification in campanulid angiosperms. *Evolution* 67: 3132–3144.
- Bonhomme, V., S. Picq, C. Gaucherel, and J. Claude. 2014. Momocs: Outline analysis using R. *Journal of Statistical Software* 56: 1–24.
- Boon, J. J., S. A. Stout, W. Genuit, and W. Spackman. 1989. Molecular paleobotany of *Nyssa* endocarps. *Acta Botanica Neerlandica* 38: 391–404.
- Clement, W. L. and M. J. Donoghue. 2011. Dissolution of *Viburnum* section *Megalotinus* (Adoxaceae) of Southeast Asia and its implications for morphological evolution and biogeography. *International Journal of Plant Sciences* 172: 559–573.
- Clement, W. L., M. Arakaki, P. W. Sweeney, E. J. Edwards, and M. J. Donoghue. 2014. A chloroplast tree for *Viburnum* (Adoxaceae) and its implications for phylogenetic classification and character evolution. *American Journal of Botany* 101: 1029–1049.
- Clement, W. L., T. J. Stammer, A. Goble, P. Gallagher, and M. J. Donoghue. 2021. Data from: Parallelism in endocarp form sheds light on fruit syndrome evolution in *Viburnum*. Dryad Digital Repository. <https://doi.org/10.5061/dryad.j3tx95x1>.
- Dardick, C. and A. M. Callahan. 2014. Evolution of the fruit endocarp: Molecular mechanisms underlying adaptations in seed protection and dispersal strategies. *Frontiers in Plant Science* 5: 284.
- Depypere, L., P. C. Chaerle, K. V. Mijnsbrugge, and P. Goetghebeur. 2007. Stony endocarp dimension and shape variation in *Prunus* section *Prunus*. *Annals of Botany* 100: 1585–1597.
- Dilcher, D. L. and J. F. McQuade. 1967. A morphological study of *Nyssa* endocarps from Eocene deposits in western Tennessee. *Bulletin of the Torrey Botanical Club* 94: 35–40.
- Donoghue, M. J. 1983a. The phylogenetic relationships of *Viburnum*. Pp. 143–166 in *Advances in Cladistics*, vol. 2, eds. N. I. Platnick and V. A. Funk. New York: Columbia University Press.
- Donoghue, M. J. 1983b. A preliminary analysis of phylogenetic relationships in *Viburnum* (Caprifoliaceae s. l.). *Systematic Botany* 8: 45–58.
- Donoghue, M. J., B. G. Baldwin, J. Li, and R. C. Winkworth. 2004. *Viburnum* phylogeny based on the chloroplast *trnK* intron and nuclear ribosomal ITS DNA sequences. *Systematic Botany* 29: 188–198.
- Edgar, R. C. 2004. MUSCLE: Multiple sequence alignment with high accuracy and high throughput. *Nucleic Acids Research* 32: 1792–1797.
- Gottschling, M., D. H. Mai, and H. H. Hilger. 2002. The systematic position of *Ehretia* fossils (Ehretiaceae, Boraginales) from the European Tertiary and implications for character evolution. *Review of Palaeobotany and Palynology* 121: 149–156.
- Hara, H. 1983. *A Revision of the Caprifoliaceae of Japan with Reference to Allied Plants in Other Districts and the Adoxaceae*. Tokyo: Academica Scientifica Books Inc.
- Huelsenbeck, J. P. and F. Ronquist. 2001. MRBAYES: Bayesian inference of phylogeny. *Bioinformatics* 17: 754–755.
- Jacobs, B., M. J. Donoghue, F. Bouman, S. Huysmans, and E. Smets. 2008. Evolution and phylogenetic importance of endocarp and seed characters in *Viburnum* (Adoxaceae). *International Journal of Plant Sciences* 169: 409–431.
- Jacques, M. B. and Z. Zhou. 2010. Geometric morphometrics: A powerful tool for the study of shape evolution in Menispermaceae endocarps. *Taxon* 59: 881–895.
- Kern, J. H. 1951. The genus *Viburnum* (Caprifoliaceae) in Malaysia. *Reinwardtia* 1: 107–170.
- Koubouris, G. C., E. V. Avramidou, I. T. Metzidakis, P. V. Petrakis, C. K. Sergentani, and A. G. Doulis. 2019. Phylogenetic and evolutionary applications of analyzing endocarp morphological characters by classification binary tree and leaves by SSR markers for the characterization of olive germplasm. *Tree Genetics & Genomes* 15: 26.
- Landis, M. J., D. A. R. Eaton, W. L. Clement, B. Park, E. L. Spriggs, P. W. Sweeney, E. J. Edwards, and M. J. Donoghue. 2020. Joint phylogenetic estimation of geographic movements and biome shifts during the global diversification of *Viburnum*. *Systematic Biology* 70: 67–85.
- Lanfear, R., B. Calcott, S. Y. W. Ho, and S. Guindon. 2012. PartitionFinder: Combined selection of partitioning schemes and substitution models for phylogenetic analyses. *Molecular Biology and Evolution* 29: 1695–1701.
- Lens, F., R. A. Vos, G. Charrier, T. van der Niet, V. Merckx, P. Bass, J. A. Gutierrez, B. Jacobs, L. C. Doria, E. Smets, S. Delzon, and S. B. Janssens. 2016. Scalariform-to-simple transition in vessel perforation plates triggered by differences in climate during the evolution of Adoxaceae. *Annals of Botany* 118: 1043–1056.
- Li, Y., T. Smith, C.-J. Liu, N. Awasthi, J. Yang, Y.-F. Wang, and F.-S. Li. 2011. Endocarps of *Prunus* (Rosaceae: Prunoideae) from the early Eocene of Wutu, Shandong Province, China. *Taxon* 60: 555–564.
- Maddison, W. P. and D. R. Maddison. 2019. Mesquite: A modular system for evolutionary analysis. Version 3.51. <http://www.mesquiteproject.org>.
- Oersted, A. S. 1861. Til belysning af slægten *Viburnum*. Videnskabelige Meddelelser fra Dansk Naturhistorisk Forening I Kjøbenhavn 13: 267–305.
- Ollerton, J., R. Alarcón, N. M. Waser, M. V. Price, S. Watts, L. Cranmer, A. Hingston, C. I. Peter, and J. Rotenberry. 2009. A global test of the pollination syndrome hypothesis. *Annals of Botany* 103: 1471–1480.
- Paradis, E., J. Claude, and K. Strimmer. 2004. APE: Analyses of phylogenetics and evolution in R language. *Bioinformatics* 20: 289–290.
- Plunkett, G. M., D. E. Soltis, and P. S. Soltis. 1996. Evolutionary patterns in Apiceae: Inferences based on *matK* sequence data. *Systematic Botany* 21: 477–495.
- R Core Team. 2019. R: A language and environment for statistical computing. Vienna, Austria: R Foundation for Statistical Computing. <https://www.R-project.org/>.

- Rambaut, A., A. J. Drummond, D. Xie, G. Baele, and M. A. Suchard. 2018. Posterior summarization in Bayesian phylogenetics using Tracer 1.7. *Systematic Biology* 67: 901–904.
- Rehder, A. 1940. *Manual of Cultivated Trees and Shrubs*. New York: Macmillan.
- Revell, L. J. 2012. phytools: An R package for phylogenetic comparative biology (and other things). *Methods in Ecology and Evolution* 3: 217–223.
- Ronquist, F. and J. P. Huelsenbeck. 2003. MrBayes 3: Bayesian phylogenetic inference under mixed models. *Bioinformatics* 19: 1572–1574.
- Rosas-Guerrero, V., R. Aguilar, S. Martín-Rodríguez, L. Ashworth, M. Lopezaraiza-Mikel, J. M. Bastida, and M. Quesada. 2014. A quantitative review of pollination syndromes: Do floral traits predict effective pollinators? *Ecology Letters* 17: 388–400.
- Rozefelds, A. and D. C. Christophel. 1996. *Elaeocarpus* (Elaeocarpaceae) endocarps from the oligo-miocene of eastern Australia. *Papers and Proceedings of the Royal Society of Tasmania* 130: 41–48.
- Sattarian, A. and L. J. G. van der Maesen. 2006. Endocarp morphology of African *Celtis* (Celtidaceae/Ulmaceae). *Blumea* 51: 389–397.
- Sinnott-Armstrong, M. A., C. Lee, W. L. Clement, and M. J. Donoghue. 2020. Fruit syndromes in *Viburnum*: Correlated evolution of color, nutritional content, and morphology in bird-dispersed fleshy fruits. *BMC Evolutionary Biology* 20: 1–19.
- Spriggs, E. L., W. L. Clement, P. W. Sweeney, S. Madriñan, E. J. Edwards, and M. J. Donoghue. 2015. Temperate radiations and dying embers of a tropical past: The diversification of *Viburnum*. *The New Phytologist* 207: 340–354.
- Stayton, C. T. 2015. The definition, recognition, and interpretation of convergent evolution, and two new measures for quantifying and assessing the significance of convergence. *Evolution* 69: 2140–2153.
- Thiers, B. 2020. Index Herbariorum: A global directory of public herbaria and associated staff. New York Botanical Garden's Virtual Herbarium. <http://sweetgum.nybg.org/ih/> (last accessed Oct 2020).
- Van der Pijl, L. 1969. *Principles of Dispersal in Higher Plants*. Berlin: Springer.
- Wefferling, K. M., S. B. Hoot, and S. S. Neves. 2013. Phylogeny and fruit evolution in Menispermaceae. *American Journal of Botany* 100: 883–905.
- Wilkinson, A. M. 1948. Floral anatomy and morphology of some species of the genus *Viburnum* of the Caprifoliaceae. *American Journal of Botany* 35: 455–465.
- Winkworth, R. C. and M. J. Donoghue. 2005. *Viburnum* phylogeny based on combined molecular data: Implications for taxonomy and biogeography. *American Journal of Botany* 92: 653–666.
- Yang, Q.-E. and V. Malécot. 2011. *Viburnum*. Pp. 570–611 in *Flora of China*, vol. 19, eds. Z.-Y. Wu, P. H. Raven, and D. Y. Hong. Beijing and St. Louis: Science Press/Missouri Botanical Garden Press.
- Zhang, H. and Z. Zhang. 2008. Endocarp thickness affects seed removal speed by small rodents in a warm-temperate broad-leaved deciduous forest, China. *Acta Oecologica* 34: 285–293.
- Zwickl, D. J. 2006. Genetic Algorithm Approaches for the Phylogenetic Analysis of Large Biological Sequence Datasets Under the Maximum Likelihood Criterion. Ph.D. thesis. Austin, Texas: The University of Texas at Austin.
- APPENDIX 1. Voucher information and GenBank accession numbers for all plant material used in phylogenetic analyses and studies of endocarp morphology. Species are arranged alphabetically and missing data are indicated with a dash (–). For each species, the following information is provided: voucher specimen for molecular work, herbarium, GenBank accession numbers for *matK*, *ndhF*, *petB-petD*, *rbcL*, *rpl32-trnL*^(UAG), *trnC-ycf6*, *trnH-psbA*, *trnK*, *trnS-trnG*, ITS; voucher specimen for morphological work, herbarium, specimen type (CL = camera lucida drawing; H = herbarium; P = pickled). Herbarium abbreviations follow Index Herbariorum (Thiers 2020) and NVI refers to no voucher information.
- V. acerifolium* L., M.J. Donoghue & R.C. Winkworth 27, YU, HQ591557, HQ591641, HQ591987, HQ591701, HQ591863, HQ592108, AY627384, AY265160, HQ591819, AY265114; C.G. Pringle 207, A, H. V. *adenophorum* W.W.Smith, D.E. Boufford & B. Bartholomew 24402, A, HQ591558, –, HQ591988, HQ591702, HQ591864, HQ592109, HQ592057, HQ591781, MT025847, HQ591948; D.E. Boufford & B. Bartholomew 24803, A, H. V. *amplifolium* Rehder, P.W. Sweeney et al. 2252, YU, MN914753, MN937378, MN987749, MN937409, MN987905, MN987683, MN987817, MN987865, MN987633, MN952543; H.T. Tsai 61436, A, CL. V. *atrocyaneum* C.B. Clarke, D.E. Boufford et al. 34956, A, HQ591559, HQ591642, HQ591989, HQ591703, HQ591866, HQ592110, HQ592059, HQ591782, HQ591820, HQ591950; K.M. Feng 3054, A, CL. V. *australe* Morton, M.A. Carranza et al. 2064, MO, JQ805235, –, –, JQ805393, –, KP281879, JQ805304, KP281896, –, JQ805157; M.J. Donoghue 2, YU, H. V. *awabuki* K.Koch, S.-M. Liu et al. 141, A, HQ591560, –, HQ591990, HQ591704, HQ591867, HQ592111, HQ592060, HQ591783, –, HQ591951; Walker et al. 6058, A, CL. V. *betulifolium* Batalin, P.W. Sweeney et al. 2344, YU, MN914760, MN937385, MN987756, MN937416, MN987912, MN987690, MN987824, MN987872, MN987640, MN952550; B. Bartholomew et al. 1415, A, CL. V. *bitchiuense* Makino, D. Chatelet 1097-77A, Arnold Arboretum living collection, JX049451, JX049459, JX049509, JX049471, JX049477, JX049481, JX049467, JX049491, JX049495, JX049448; NVI, CL. V. *blandum* C.V.Morton, M.J. Donoghue 464, YU, HQ591562, –, HQ591992, HQ591706, HQ591869, HQ592113, HQ592062, HQ591785, –, HQ591952; M.J. Donoghue 339, YU, H. V. *brachybotryum* Hemsl. Et F.B.Forbes & Hemsl., P.W. Sweeney et al. 2222, YU, MN914761, MN937386, MN987757, MN937417, MN987913, MN987691, MN987825, –, MN987641, MN952551; E.H. Wilson 1840, A, CL. V. *buddleifolium* C.H.Wright, P.W. Sweeney et al. 2607, YU, MN914762, MN937387, MN987758, MN937418, MN987914, MN987692, MN987826, MN987873, MN987642, MN952552; E.H. Wilson 1838, A, CL. V. *burejaeticum* Regel & Herder, K. Schmandt 375-95A/00223095, A, JQ805231, JX049463, JX049513, JX049463, JX049473, JQ805472, JX049486, JQ805297, JQ805552, JX049500, –, P.H. Dorsett 4204, A, CL. V. *calvum* Rehder, H. Li & V. Soukup 934, A, HQ591565, HQ591644, HQ591995, HQ591709, HQ591872, HQ592116, HQ592066, HQ591788, JX049508, HQ591955; H.T. Tsai 52358, A, CL. V. *carlesii* Hemsl. ex Forb. & Hemsl., M.J. Donoghue & R.C. Winkworth 24, YU, HQ591566, HQ591645, HQ591996, HQ591710, HQ591873, HQ592117, AY627385, AY265161, HQ591823, AY265115; E.H. Wilson 10601, A, CL. V. *cassinooides* L., E.L. Spriggs 79, YU, MN914763, MN937388, MN987759, MN937419, MN987915, MN987693, MN987827, –, MN987643, MN952553; ELS 232 YU, E.L. Spriggs 408 A, H. V. *caudatum* Greenm., M.J. Donoghue 64, YU, –, –, –, HQ591875, HQ592119, HQ592068, HQ591790, HQ591825, HQ591957; M.J. Donoghue 38, YU, H. V. *chingii* P.S.Hsu, P.W. Sweeney et al. 2247, YU, MN914764, MN937389, MN987760, MN937420, MN987916, MN987694, MN987828, MN987874, MN987644, MN952554; B. Bartholomew et al. 1379, A, CL. V. *ciliatum* Greenm., M.J. Donoghue 48, YU, JQ805240, –, MT025838, JQ805401, MT025851, MT025841, JQ805311, JQ805563, –, –, NVI, CL. V. *cinnamomifolium* Rehder, P.W. Sweeney et al. 2255, YU, MN914765, MN937390, MN987761, MN937421, MN987917, MN987695, MN987829, MN987875, MN987645, MN952555; NVI, CL. V. *clomensiae* Kern, J. Beauman 11781, K, HQ591569, HQ591648, HQ591999, HQ591714, HQ591878, HQ592122, AY627387, AY265163, EF490267, AY265117; P.W. Sweeney et al. 2145, YU, H. V. *congestum* Rehder, P.W. Sweeney et al. 2235, YU, MN914754, MN937379, MN987750, MN937410, MN987906, MN987684, MN987818, MN987866, MN987634, MN952544; P.W. Bristol 42, A, CL. V. *coriaceum* Bl., P.W. Sweeney et al. 2088, YU, KP281810, KP281828, KP281864, KP281818, KP281854, KP281876, KP281845, KP281893, KP281902, KP281840; M. Balgooy, K. W. Radianata 2890, A, H. V. *costaricanum* Hemsl., M.J. Donoghue 85, YU, –, KP281831, –, –, JQ805482, –, –, JQ805564, KF019909, JQ805164; M.J. Donoghue 645, YU, H. V. *cotinifolium* D.Don, M.J. Donoghue WC267, YU, KF019744, KF019767, KF019823, KF019787, KF019864, –, KF019843, KF019932, KF019908, KF019809; R.R. Stewart 17253, A, CL. V. *cylindricum* Buch.-Ham. ex D.Don, P.W. Sweeney et al. 2233, YU, MN914766, MN937391, MN987762, MN937422, MN987918, MN987696, MN987830, MN987876, MN987646, MN952556; H.T. Tsai 59828, A, CL. V. *davidii* Franch., M.J. Donoghue WC269, YU, KF019765, KF019785, KF019841, KF019807, KF019883, KF019906, KF019862, KF019951, KF019930, KF019821; E.H. Wilson 963, A, CL. V. *dentatum* L., M.J. Donoghue & R.C. Winkworth 33, YU, HQ591574, HQ591651, HQ592002, HQ591718, HQ591884, HQ592128, AY627391, AY265167, HQ591827, AY265121; F.W. Hunnewell 4551, GH, CL. V. *dilatatum* Thunb., P.W. Sweeney et al. 2209, YU, MN914767, MN937392, MN987763, MN937423, MN987919, MN987697, MN987831, –, MN987647, –, I. Hurusawa 1418, A, CL. V. *discolor* Benth., M. Veliz, N. Gallardo, M. Vasquez 35-99, MO, JQ805241, –, –, JQ805402, JQ805485, KF019886, JQ805314, MT025846, –, JQ805166; M.J. Donoghue 507, YU, CL. V. *disjunctum* C.V.Morton, M.J. Donoghue 700, YU, KF019745, –, –, KF019788, –, KF019887, KF019844, –, KF019910, KF019810; M.J. Donoghue 492, YU, H. V. *edule* (Michx.) Raf., NVI, HQ591577, –, –, HQ591720, –, –, AY627393, AY265169, EF490271, AY265123; M.C. Fernald, L.B. Smith 26029, GH, CL. V. *elatum* Benth., P.W. Sweeney et al. 3063, YU, MN914768, MN937393, MN987764, MN937424, MN987920, –, MN987832, –, MN987648, MN952557; NVI, CL. V. *ellipticum* Hook., M.J. Donoghue NVI, HQ591579, HQ591653, HQ592004, HQ591722, –, HQ592131, AY627395, AY265171, HQ591830, AY265125; W.N. Suksdorf 6119, A, CL. V. *erosum* Thunb., M.J. Donoghue et al. 4, YU, MN914769, MN937394, MN987765, MN937425, MN987921,

- MN987698, MN987833, MN987877, MN987649, –; *M. Togasi* 649, *H. Muroi* 6069, *A. CL. V. erubescens* Wall., *Boufford et al.* 27190, *A.*, HQ591581, HQ591655, HQ592006, HQ591724, HQ591889, HQ592133, AY627397, AY265173, HQ591831, AY265127; *J.F. Rock* 6847, *E.H. Wilson* 305, *A. CL. V. flavescens* W.W.Smith, *Boufford et al.* 32758, *A.*, HQ591583, HQ591657, HQ592008, HQ591726, HQ591891, –, HQ592074, HQ591794, JX049505, HQ591962; *K.M. Feng* 2921, *A.*, *H. V. foetens* Decne., *M.J. Donoghue* WC270, *YU.*, KF019754, KF019774, KF019831, KF019796, KF019872, KF019895, KF019851, KF019940, KF019919, KF019813; *Shahzad et al.* 113, *A. CL. V. foetidum* Wall., *M.J. Donoghue & K-F. Chung* KFC1942, *YU.*, KF019759, KF019779, KF019835, KF019801, KF019877, KF019900, KF019856, KF019945, KF019924, KF019818; *H.F. Handel-Mazzetti* 771, *A. CL. V. fordiae* Hance, no molecular data; *W.Y. Chun* 5224, *A. CL. V. formosanum* Hayata, *M.J. Donoghue & J.M. Hu* J-M Hu 2007, *YU.*, KF019760, KF019780, KF019836, KF019802, KF019878, KF019901, KF019857, KF019946, KF019925, –; *B. Bartholomew et al.* 434 *A.*, *H. V. glaberrimum* Merr., *P.W. Sweeney et al.* 2322, *YU.*, MN914755, MN937380, MN987751, MN937411, MN987907, MN987685, MN987819, MN987867, MN987635, MN952545; *M. Jacobs* 7434, *A. CL. V. glomeratum* Maxim., *P.W. Sweeney et al.* 2559, *YU.*, MN914770, MN937395, MN987766, MN937426, MN987922, MN987699, MN987834, MN987878, MN987650, MN952558; *J. Hers* 2782, *A. CL. V. grandiflorum* Wall. ex DC, *M.J. Donoghue* WC271, *YU.*, KF019755, KF019775, KF019832, KF019797, KF019873, KF019896, KF019852, KF019941, KF019920, KF019814; *S. Noshiro, N. Fujii, T. Kajita, K. Yoda* 9480199, *A.*, *H. V. hallii* Killip & A.C.Smith, *P.W. Sweeney et al.* 1626, *YU.*, JQ805248, –, MT025839, JQ805410, JQ805492, MT025842, JQ805327, JQ805572, MT025848, JQ805173; *P.W. Sweeney et al.* 1825, *YU.*, *H. V. hanceanum* Maxim., *P.W. Sweeney et al.* 2195, *YU.*, MN914756, MN937381, MN987752, MN937412, MN987908, MN987686, MN987820, MN987868, MN987636, MN952546; *W.Y. Chun* 7173, *A.*, *H. V. hartwegii* Benth., *M.J. Donoghue* 40, *YU.*, HQ591586, HQ591659, HQ592011, –, HQ591894, HQ592137, AY627400, AY265176, HQ591832, AY265130; *M.J. Donoghue* 672, *YU.*, *H. V. hebanthum* Wight & Arn., *J. Klackenberg* 32, *NY.*, HQ591587, HQ591660, HQ592012, HQ591729, HQ591895, HQ592138, HQ592076, HQ591795, HQ591833, –; *E.H. Wilson s.n.*, *A. CL. V. henryi* Hemsl., *M.J. Donoghue* WC272, *YU.*, KF019756, KF019776, –, KF019798, KF019874, KF019897, KF019853, KF019942, KF019921, KF019815; *Fang* 2473, *A. CL. V. hondurensis* Standl., no molecular data; *Lopez* 67, *GH.*, *H. V. hupehense* Rehder, *Bartholomew et al.* 1286, *A.*, HQ591588, HQ591661, HQ592013, HQ591730, HQ591896, HQ592139, HQ592077, HQ591796, HQ591834, HQ591964; *E.H. Wilson* 237, 1025, *A. CL. V. ichangense* Rehder, *Bartholomew et al.* 1889, *A.*, HQ591589, HQ591662, HQ592014, HQ591731, HQ591897, HQ592140, HQ592078, HQ591797, HQ591835, HQ591965; *E.H. Wilson* 221, *B. Bartholomew et al.* 446, *A. CL. V. inopinatum* Craib., *P.W. Sweeney et al.* 2091, *YU.*, KF019750, KF019770, KF019827, KF019792, KF019868, KF019891, KF019847, KF019936, KF019915, KJ795808; *J.F. Maxwell* 89-1444, *A.*, *H. V. integrifolium* Hayata, *M.J. Donoghue & K-F. Chung* KFC1946, *YU.*, KF019761, KF019781, KF019837, KF019803, KF019879, KF019902, KF019858, KF019947, KF019926, –; *K-F. Chung* 1945, *YU.*, *H. V. japonicum* Spreng, *NVI.*, *YU.*, HQ591592, HQ591664, HQ592016, HQ591733, HQ591899, HQ592143, AY627401, AY265177, HQ591837, AY265131; *Maximowicz* 1863, *A. CL. V. jucundum* C.V.Morton, *M.J. Donoghue* 244, *YU.*, HQ591593, HQ591665, HQ592017, HQ591734, HQ591900, –, AY627402, AY265178, HQ591838, AY265132; *M.J. Donoghue* 309, *YU.*, *H. V. kansuense* Batalin, *Boufford et al.* 27416, *A.*, HQ591594, HQ591666, HQ592018, HQ591735, HQ591901, HQ592144, AY627403, AY265179, EF490276, AY265133; *D.E. Boufford, M.J. Donoghue, R.H. Ree* 27348, *A.*, *H. V. lantana* L., *M.J. Donoghue & R.C. Winkworth* 26, *YU.*, HQ591595, HQ591667, HQ592019, HQ591736, HQ591902, HQ592145, AY627404, AY265180, EF490278, AY265134; *D.P. Nikolaeo, T.N. Medvedeo s.n.*, *A.*, *H. V. lantanoideis* Michx., *M.J. Donoghue & R.C. Winkworth* 2, *YU.*, HQ591596, HQ591668, HQ592020, HQ591737, HQ591903, HQ592146, AY627405, AY265181, EF490279, AY265135; *S.H. Burnham s.n.*, *GH.*, *CL. V. lasiophyllum* Benth., *P.W. Sweeney et al.* 2174, *YU.*, KP281814, KP281834, KP281869, KP281822, KP281859, KP281884, KP281849, –, KP281907, –, *P.W. Sweeney et al.* 2174, *YU.*, *V. lautum* C.V.Morton, *M.J. Donoghue* 72, *YU.*, HQ591597, HQ591669, HQ592021, HQ591738, HQ591904, HQ592147, HQ592082, HQ591799, HQ591839, HQ591967; *M.J. Donoghue* 103, *YU.*, *H. V. leiocarpum* P.S.Hsu, *P.W. Sweeney et al.* 2265, *YU.*, MN914757, MN937382, MN987753, MN937413, MN987909, MN987687, MN987821, MN987869, MN987637, MN952547; *K.M. Feng* 13870, *A.*, *H. V. lentago* L., *M.J. Donoghue & R.C. Winkworth* 21, *YU.*, HQ591598, HQ591670, HQ592022, HQ591739, HQ591905, HQ592148, AY627406, AY265182, EF490280, AY265136; *Whetzel* 12955 *GH.*, *H. V. lepidotulum* Merr. & Chun, *P.W. Sweeney et al.* 2097, *YU.*, KF019748, KF019768, KF019825, KF019790, KF019866, KF019889, –, KF019934, KF019913, KJ795805; *P.W. Sweeney et al.* 2101, *YU.*, *H. V. lobophyllum* Graebn., *M.J. Donoghue & R.C. Winkworth* 25, *YU.*, HQ591600, HQ591671, HQ592023, HQ591741, HQ591907, HQ592149, AY627407, AY265183, HQ591840, AY265137; *B. Bartholomew et al.* 1416, *A.*, *CL. V. loeseneri* Graebn., *M.J. Donoghue* 2547, *YU.*, HQ591601, –, HQ592024, HQ591742, HQ591908, HQ592150, HQ592084, HQ591801, –, HQ591968; *M.J. Donoghue* 2547, *YU.*, *H. V. lutescens* Bl., *P.W. Sweeney et al.* 2077, *YU.*, MN914771, MN937396, MN987767, MN937427, MN987923, MN987700, –, MN987879, MN987651, MN952559; *NVI.*, *CL. V. luzonicum* Rolfe, *P.W. Sweeney et al.* 2321, *YU.*, MN914772, MN937397, MN987768, MN937428, MN987924, MN987701, MN987835, –, MN987652, –, *Hu* 2008, *YU.*, *H. V. macrocephalum* Fortune, *M.J. Donoghue* 101, *YU.*, HQ591604, HQ591673, HQ592027, HQ591745, HQ591911, HQ592153, HQ592086, EF490247, HQ591842, EF462984; *Macgregor s.n.*, *A. CL. V. microcarpum* Schlecht. & Cham., *F. Ventura* A. 819, *NY.*, –, –, –, JQ805414, JQ805496, –, JQ805327, KP281898, –, JQ805178; *M.J. Donoghue* 32, *YU.*, *H. V. molle* Michx., *M.J. Donoghue & R.C. Winkworth* 5, *YU.*, HQ591606, HQ591675, –, HQ591747, HQ591913, HQ592154, AY627409, AY265185, EF490281, AY265139; *E.J. Palmer* 26158, *A.*, *CL. V. mongolicum* Rehder, *M.J. Donoghue s.n.*, *YU.*, HQ591607, HQ591676, HQ592029, HQ591748, HQ591914, HQ592155, HQ592087, EF490248, HQ591844, EF462985; *Teng* 1383, *A. CL. V. mullaha* Buch-Ham. ex D.Don, *M.J. Donoghue* WC274, *YU.*, KF019762, KF019782, KF019838, KF019804, KF019880, KF019903, KF019859, KF019948, KF019927, KF019819; *H. Hara et al.* 6302997, *A.*, *CL. V. nervosum* D.Don, *P.W. Sweeney et al.* 2298, *YU.*, MN914773, MN937398, MN987769, MN937429, MN987925, MN987702, MN987836, MN987880, MN987653, MN952560; *A.J.C. Grierson, D.G. Long* 2805, *A.*, *CL. V. nudum* L., *E.L. Spriggs* 29, *YU.*, MN914774, MN937399, MN987770, MN937430, MN987926, MN987703, MN987837, MN987881, MN987654, MN952561; *M.L. Fernald et al.* 15360, *GH.*, *CL. V. obovatum* Walter, *E.L. Spriggs* 264, *YU.*, MN914758, MN937383, MN987754, MN937414, MN987910, MN987688, MN987822, MN987870, MN987638, MN952548; *R.K. Godfrey, R.M. Tryon* 8215, *GH.*, *CL. V. obtusatum* D.N.Gibson, *P.W. Sweeney et al.* 3100, *YU.*, MN914775, MN937400, MN987771, MN937431, MN987927, MN987704, MN987838, –, MN987655, MN952562; *M.J. Donoghue* 2359, *YU.*, *H. V. odoratissimum* Ker-Gawl., *R. Olmstead* 118, *WTU.*, HQ591609, HQ591678, –, HQ591750, HQ591916, HQ592157, AY627411, AY265187, HQ591845, AY265141; *W.T. Tsang* 25600, *A. CL. V. oliganthum* Batalin, *D.E. Boufford et al.* 27175, *A.*, HQ591610, –, –, HQ591751, HQ591917, HQ592158, HQ592088, HQ591804, HQ591846, HQ591971; *E.H. Wilson* 805, *A. CL. V. opulus* L., *W.L. Clement* 250, *YU.*, HQ591611, HQ591679, –, HQ591752, HQ591918, HQ592159, –, HQ591805, HQ591847, HQ591972; *L. Holm-Nielsen et al.* 222, *A. CL. V. orientale* Pall., *Merello et al.* 2291, *MO.*, HQ591612, HQ591680, HQ592031, HQ591753, HQ591919, HQ592160, HQ592089, EF490249, EF490284, EF462986; *R.E. Regel s.n.*, *A. CL. V. ovatifolium* Rehder, no molecular data; *E.H. Wilson* 240, *A.*, *CL. V. pastasanum* Diels, *P.W. Sweeney et al.* 1799, *YU.*, HQ591634, HQ591694, HQ592050, HQ591774, HQ591941, HQ592181, HQ592103, HQ591814, HQ591858, HQ591982; *Neill* 13547, *YU.*, *H. V. phlebotrichum* Siebold & Zucc., *M.J. Donoghue et al.* 3, *YU.*, MN914759, MN937384, MN987755, MN937415, MN987911, MN987689, MN987823, MN987871, MN987639, MN952549; *Mizushima* 2930, *A. CL. V. pichinchense* Benth., *P.W. Sweeney et al.* 1669, *YU.*, JQ805257, KP281835, KP281870, JQ805420, JQ805502, KP281886, JQ805332, JQ805580, –, JQ805184; *Croat* 98333, *YU.*, *H. V. plicatum* Thunb., *M.J. Donoghue & R.C. Winkworth* 10, *YU.*, HQ591613, HQ591681, HQ592032, HQ591754, HQ591920, HQ592161, AY627412, AY265189, EF490285, AY265143; *Gressitti* 1472, *A.*, *CL. V. propinquum* Hemsl., *P.W. Sweeney et al.* 2188, *YU.*, MN914776, MN937401, MN987772, MN937432, MN987928, MN987705, MN987839, MN987882, MN987656, MN952563; *E.H. Wilson* 498, *A.*, *CL. V. prunifolium* L., *M.J. Donoghue & R.C. Winkworth* 13, *YU.*, HQ591615, HQ591683, HQ592033, HQ591756, HQ591922, HQ592163, AY627413, AY265190, EF490286, AY265144; *F.D. 1076*, *A.*, *CL. V. punctatum* Buch-Ham. ex D.Don, *P.W. Sweeney et al.* 2274, *YU.*, MN914777, –, MN987773, MN937433, MN987929, MN987706, MN987840, –, MN987657, –, *Feng* 63, *A.*, *CL. V. rafinesquianum* Schult., *M.J. Donoghue & R.C. Winkworth* 4, *YU.*, HQ591617, HQ591684, HQ592035, HQ591758, HQ591924, HQ592165, AY627414, AY265191, HQ591849, AY265145; *C.E. Wood Jr.* 5599, *GH.*, *H. V. recognitum* Fernald, *Arnold Arboretum* 1471-83B/0012902, *A.*, JQ805261, JX049465, KF019824, JQ805387, JQ805507, JX049490, JQ805337, JQ805585, JX049504, JQ805189; *E. Rouleau* 1395, *GH.*, *CL. V. rhytidophyllum* Hemsl. ex Forb. & Hemsl., *M.J. Donoghue & R.C. Winkworth* 8, *YU.*, HQ591618, HQ591685, HQ592036, HQ591759, HQ591925, HQ592166, HQ592092, AY265192, HQ591850, AY265146; *E.H. Wilson*

- 220, A, CL. *V. rigidum* Vent., W.T. Stearn 1116, A, HQ591619, HQ591686, HQ592037, HQ591760, HQ591926, -, HQ592093, HQ591807, -, HQ591974; E. Bourgeau s.n., A, CL. *V. rufidulum* Raf., M.J. Donoghue & R.C. Winkworth 14, YU, HQ591620, HQ591687, HQ592038, HQ591761, HQ591927, HQ592167, AY627415, AY265193, EF490287, AY265147; S.B. Jones 23635, PH, H. V. *sambucinum* Reinw. ex Blume, P.W. Sweeney et al. 2100, YU, KF019751, KF019771, KF019828, KF019793, KF019869, KF019892, KF019848, KF019937, KF019916, KF019811; B.C. Stone 14420, R. Boea 10916, A, CL. *V. sargentii* Koehne, M.J. Donoghue & R.C. Winkworth 17, YU, HQ591621, HQ591688, HQ592039, HQ591762, HQ591928, HQ592168, AY627416, AY265194, EF490288, AY265148; B. Bartholomew et al. 1730, A, CL. *V. scabellum* Chapman, M.J. Donoghue 82, YU, JQ805262, KP281836, KP281871, KP281824, JQ805508, KP281887, JQ805338, JQ805586, KP281910, JQ805190; R.K. Godfrey, R.M. Tryon 54224, GH, CL. *V. schensianum* Maxim., P.W. Sweeney et al. 2565, YU, MN914778, MN937402, MN987774, MN937434, MN987930, MN987707, MN987841, MN987883, MN987658, MN952564; E. Licent 12633, A, H. V. *seemianii* Graebn., M. Lewis 37409, GH, JQ805263, -, -, JQ805426, JQ805509, -, JQ805340, JQ805587, -, JQ805193; A.L. Cabrera et al. 27840, PH, H. V. *sempervirens* K.Koch, P.W. Sweeney et al. 2191, YU, MN914779, MN937403, MN987775, MN937435, MN987931, MN987708, MN987842, MN987884, MN987659, MN952565; Tsang 21630, A, CL. *V. setigerum* Hance, P.W. Sweeney et al. 2554, YU, MN914780, MN937404, MN987776, MN937436, MN987932, MN987709, MN987843, MN987885, MN987660, MN952566; E.H. Wilson 236, A, CL. *V. sieboldii* Miq., M.J. Donoghue et al. 7, YU, MN914781, MN937405, MN987777, MN937437, MN987933, MT025844, MN987844, MN987886, MN987661, MN952567; Walker et al. 5658, A, CL. *V. stellato-tomentosum* Hemsl., M.J. Donoghue 640, YU, KF019747, -, -, KF019789, KF019865, KF019888, KF019845, -, KF019911, -, Hemsley 4830, GH, H. V. *stenocalyx* Hemsl., M.J. Donoghue 60, YU, HQ591626, -, HQ592043, HQ591767, HQ591933, HQ592173, HQ592097, HQ591810, KF019912, HQ591978; M.J. Donoghue 60, YU, H. V. *suspensum* Lindl., M.J. Donoghue & R.C. Winkworth 36, YU, HQ591629, HQ591692, HQ592045, HQ591769, HQ591936, HQ592176, AY627419, AY265197, HQ591854, AY265151; E.H. Wilson 1917, A, CL. *V. sympodiale* Graebn., K.F. Chung 1932, YU, MN914782, MN937406, MN987778, MN937438, MN987934, MN987710, MN987845, MN987887, MN987662, MN952568; E.H. Wilson 294, A, CL. *V. taitoense* Hayata, M.J. Donoghue & K-F. Chung KFC1941, YU, KF019757, KF019777, KF019833, KF019799, KF019875, KF019898, KF019854, KF019943, KF019922, KF019816; C.C. Chen 4200, A, H. V. *taiwanianum* Hayata, W.-H. Hu et al. 2186, MO, HQ591631, -, HQ592047, HQ591771, HQ591938, HQ592178, HQ592101, EF490253, HQ591855, EF462989; H. Keng KAO 2550, A, CL. *V. tashiroi* Nakai, M.J. Donoghue s.n., YU, KF019764, KF019784, KF019840, KF019806, KF019882, KF019905, KF019861, KF019950, KF019929, -, S. Kobayashi 2817, A, H. V. *tenguehense* (W.W.Sm.) P.S.Hsu, no molecular data; H.T. Tsai 62565, A, H. V. *ternatum* Rehder, no molecular data; W.P. Fan 3309, A, CL. *V. tiliaefolium* (Oerst.) Hemsl., no molecular data; M.J. Donoghue 123, YU, H. V. *tinoides* L., P.W. Sweeney et al. 2167, YU, KP281816, KP281838, KP281873, KP281826, KP281862, KP281889, KP281852, KP281899, KP281912, KP281843; P.W. Sweeney et al. 2167, YU, H. V. *tinus* L., M.J. Donoghue & R.C. Winkworth 35, YU, HQ591633, HQ591693, HQ592049, HQ591773, HQ591940, HQ592180, AY627420, AY265198, HQ591857, AY265152; C.H. Godet s.n., GH, CL. *V. trilobum* Marshall, Arnold Arboretum 22900A/0174487, A, HQ591635, HQ591695, HQ592051, HQ591775, HQ591942, HQ592182, HQ592104, HQ591815, EF490290, HQ591983; W.J. Cody and W.E. Kemp 14872 GH, H. V. *triphylllum* Benth., P.W. Sweeney et al. 1783, YU, HQ591636, HQ591696, HQ592052, HQ591776, HQ591943, HQ592183, HQ592105, HQ591816, HQ591859, HQ591984; P.W. Sweeney et al. 1698, YU, H. V. *tsangii* Rehder, no molecular data; T.T. Yu 18064, A, CL. *V. urceolatum* Siebold & Zucc., M.J. Donoghue NVI, HQ591637, HQ591697, HQ592053, HQ591777, HQ591944, -, AY627423, AY265201, HQ591860, AY265155; NVI, CL. *V. utile* Hemsl., P.W. Sweeney et al. 2593, YU, MN914783, MN937407, MN987779, MN937439, MN987935, MN987711, MN987846, MN987888, MN987663, MN952569; B. Bartholomew et al. 1412, A, CL. *V. veitchii* C.H.Wright, Bouffourd et al. 27597, A, HQ591639, HQ591699, HQ592055, HQ591779, HQ591946, -, HQ592106, HQ591817, HQ591861, HQ591985; B. Bartholomew et al. 374, A, CL. *V. vernicosum* Gibbs, P.W. Sweeney et al. 2123, YU, KF019752, KF019772, KF019829, KF019794, KF019870, KF019893, KF019849, KF019938, KF019917, KF019812; P.W. Sweeney et al. 2122, YU, P. V. *villosum* Sw., M.J. Donoghue 628, YU, JQ805280, -, KP281875, JQ805443, JQ805527, KP281892, JQ805357, JQ805600, -, -, M.J. Donoghue 631, YU, H. V. *wrightii* Miq., M.J. Donoghue et al. 1, YU, MN914784, MN937408, MN987780, MN937440, MN987936, MN987712, MN987847, MN987889, MN987664, MN952570; Muir 6348, A, CL.